REPORT DOCUMENTATION PAGE

Form Approved
OMB No. 0704-0188

1. REPORT DATE *(DD-MM-YYYY)*	2. REPORT TYPE	3. DATES COVERED *(From - To)*
7 Aug 1975	Conference paper	

4. TITLE AND SUBTITLE

FLIR Performance Modeling and its Dependence upon Climatology and Meteorology

5a. CONTRACT NUMBER

5b. GRANT NUMBER

5c. PROGRAM ELEMENT NUMBER

6. AUTHOR(S)

Paul M. Moser

5d. PROJECT NUMBER

5e. TASK NUMBER

5f. WORK UNIT NUMBER

7. PERFORMING ORGANIZATION NAME(S) AND ADDRESS(ES)

Naval Air Development Center
Warminster, PA

8. PERFORMING ORGANIZATION REPORT NUMBER

9. SPONSORING/MONITORING AGENCY NAME(S) AND ADDRESS(ES)

Naval Research Laboratory
Washington, DC

10. SPONSOR/MONITOR'S ACRONYM(S)

11. SPONSOR/MONITOR'S REPORT NUMBER(S)

12. DISTRIBUTION/AVAILABILITY STATEMENT

Distribution Statement A. Approved for public release. Distribution is unlimited.

13. SUPPLEMENTARY NOTES

Presented at the Navy Electro-Optics/Meteorology Seminar held in Washington, DC on 7 Aug 1975.

14. ABSTRACT

In this presentation I shall address primarily the meteorologists and climatologists in this rather heterogeneous group and assume that the FLIR and modeling experts are here only to keep me honest. Some of the questions that I hope to answer are: What is a "FLIR"? What is FLIR performance modeling? Why is FLIR modeling important? What are the ingredients that go into a FLIR mathematical modeling exercise? What deficiencies (particularly in the fields of meteorology and climatology) exist in the available information needed to satisfy such a model? How can these deficiencies be relieved? FLIR is an acronym (not a very good one) for "Forward Looking InfraRed" which was first coined about 11 years ago to distinguish this relatively new class of airborne equipments from an earlier generation of infrared imaging devices that look primarily in a downward direction. A FLIR functions as a sort of television camera that can see in absolute darkness. It is usually mounted on gimbals in the forward part of an airplane in such a manner that the operator can aim it in any desired direction - typically forward. A FLIR performance model may be defined ideally, as a mathematical description of a FLIR and of all the relevant environmental, operational, and human factors that affect its performance.

15. SUBJECT TERMS

16. SECURITY CLASSIFICATION OF:			17. LIMITATION OF ABSTRACT	18. NUMBER OF PAGES	19a. NAME OF RESPONSIBLE PERSON
a. REPORT	b. ABSTRACT	c. THIS PAGE			19b. TELEPHONE NUMBER *(Include area code)*
U	U	U	UU	45	

FLIR PERFORMANCE MODELING AND ITS DEPENDENCE UPON CLIMATOLOGY AND METEOROLOGY

by
Paul M. Moser

I. INTRODUCTION

In this presentation I shall address primarily the meteorologists and climatologists in this rather heterogeneous group and assume that the FLIR and modeling experts are here only to keep me honest.

Some of the questions that I hope to answer are: What is a "FLIR"? What is FLIR performance modeling? Why is FLIR modeling important? What are the ingredients that go into a FLIR mathematical modeling exercise? What deficiencies (particularly in the fields of meteorology and climatology) exist in the available information needed to satisfy such a model? How can these deficiencies be relieved?

FLIR is an acronym (not a very good one) for "Forward Looking InfraRed" which was first coined about 11 years ago to distinguish this relatively new class of airborne equipments from an earlier generation of infrared imaging devices that look primarily in a downward direction. A FLIR functions as a sort of television camera that can see in absolute darkness. It is usually mounted on gimbals in the forward part of an airplane in such a manner that the operator can aim it in any desired direction - typically forward.

A FLIR performance model may be defined ideally, as a mathematical description of a FLIR and of all the relevant environmental, operational, and human factors that affect its performance.

II. FLIR CHARACTERISTICS AND APPLICATIONS

A FLIR may be defined as a mechanically scanned real-time passive imaging device that produces a television-like moving picture representation of a scene under observation by detecting the infrared radiation that all objects emit as a function of their absolute temperatures and/or by detecting the infrared radiation emitted by other sources and reflected off the objects of interest. That is, a FLIR produces thermal pictures in which, typically,

warm objects appear bright and cool objects appear dark. For example, a FLIR picture of a ship at night would show the hot stacks and engine areas glowing brightly in the dark whereas other areas such as decks cooled by the night air might exhibit temperatures lower than the water temperature and thus appear dark. Some idea of the magnitudes of these temperatures is gained by considering the following measurements made aboard a destroyer on one occasion: water temperature, 29°C; forward stack, 40°C; after stack, 34°C; bridge, 23°C; torpedo deck 22°C; forward gun, 23°C. In the absence of atmospheric transmission losses, a typical FLIR can resolve large-area target temperature differences of a few tenths of a degree. Thus, when the atmosphere is quite transparent, the above-mentioned ship target details can be detected over considerable ranges; if, however, the atmospheric transmission over the path of interest were only about 5%, the FLIR would be unable to resolve the internal detail of the ship (in the example cited) and would be able to detect only the hot stacks and perhaps the cold hull against the sea background. The nominal angular resolution of current FLIRs ranges from roughly 0.1 milliradian to 1.0 milliradian. The total angular field of view of a FLIR is typically 200 to 400 times greater than its nominal angular resolution. There are all sorts of tradeoffs involved in the design of these devices. If very high resolution (say, 0.1 milliradian) is needed, then one is pretty much restricted to a very narrow field of view (i.e., of the order of 1° to 2°) and the stabilizing and pointing of the set may become a limiting problem. If relatively low resolution (e.g., 1.0 milliradian) is acceptable, a larger total field of view (perhaps 20°) is feasible. Most FLIRs designed for airborne use have dual infrared telescopes that permit the observer to operate in a wide field-of-view, low-resolution mode for navigation and wide-area search and then to switch to the narrow field-of-view, high resolution mode for target identification.

Most of the FLIRs developed thus far have been for air-to-surface applications. The Navy uses them in its P-3 and S-3A patrol and anti-submarine warfare aircraft for ocean surveillance and is equipping its A-6E and A-7E attack aircraft with FLIRs for use in target detection, tracking and identification, and for weapon launching. They are used as navigation aids and for aircraft pilotage (terrain and obstacle avoidance) under night/adverse weather conditions. FLIRs saw extensive use in the Vietnam conflict in which they were used to detect vehicles on roads at night and to aim guns at them.

Although FLIRs are generally thought of as devices for seeing in the dark, I believe that their daytime applications have not been fully appreciated with respect to their ability to see through thin clouds, battlefield dust, industrial smoke and haze, and to recognize visually camouflaged targets.

Because FLIRs operate at wavelengths of about 10 micrometers (about 20 times the wavelength of visible light), they are less bothered by atmospheric transmission losses resulting from the scattering of radiation by the small aerosol particles that we associate with haze than are devices operating in the visible part of the spectrum. That is, if the aerosol particles are small in comparison with a wavelength, the radiation passes through with relative ease; if the particles are larger than one wavelength significant scattering and absorption losses occur.

On the other hand, FLIRs suffer disadvantages when used in atmospheres characterized by a combination of high relative humidity and high temperature (i.e., high absolute humidity). Although the atmosphere may be quite clear visually, FLIR performance may be degraded considerably because of molecular absorption by the water vapor in the atmosphere.

III. FLIR PERFORMANCE MODEL APPLICATIONS

A mathematical formalism that interrelates target characteristics, target range, properties of the atmosphere, FLIR design parameters, FLIR laboratory performance parameters, and the ability of an observer to extract from a FLIR display, the information required to perform tasks of target acquisition, classification and identification can be an important tool in the following areas:

A. Sensor Selection/Development/Production Decisions

Mathematical models enable one to evaluate the worthwhileness of FLIR versus and in conjunction with other sensors, such as low light level television and radar, before embarking on costly development and production programs.

B. FLIR Design Tool

A mathematical model enables one to make informal technical decisions regarding choices of spectral bands. There are several transmission "windows" of interest in the atmosphere. One, for example, covers roughly the wavelength interval from 8 to 13 micrometers; another, from 3 to 5.5 micrometers. The question is, "Which should we

use?" Perhaps we should design FLIRs to operate in both bands with the final choice depending upon the environmental conditions at the time and place of use. Another question is, "What are the optimum cut-on and cut-off wavelengths for a particular chosen band (e.g., 8.1 - 12.1 micrometers versus 7.6 - 12.2 micrometers)?" Generally, in the design of a FLIR we can trade off angular resolution for sensitivity and attempt to arrive at some optimum combination for the particular types and ranges of targets of interest and the environmental conditions anticipated. Knowledge of climatic and weather conditions is a key ingredient in making a FLIR model work to answer such questions reliably. To illustrate the point, we might ask, "Why develop a FLIR with resolution good enough to classify a ship at a range of, say, 20 miles if atmospheric water vapor or clouds will limit performance to, say, 5 miles 95% of the time?"

C. Sensor Evaluation

A mathematical model enables one to extrapolate relatively meager test data from a limited number of test sites to world-wide and throughout-the-year situations. The model also serves as a data management tool in calling attention to what variables should be deployed where and when. For example, models tell us that perhaps we should use 8-13 micrometer FLIRs in the artic and subarctic regions throughout the year and in the mid-latitudes in the winter time, but that perhaps we should deploy 3 to 5.5 micrometer FLIRs or low light level television in semi-tropical and tropical regions where there are large amounts of water vapor in the atmosphere.

D. Tactical Mission Planning

In an operational situation, a mathematical model would enable mission planners to select an optimum mix of weapons and sensors as a function of the environmental conditions at the time in the local area of interest. A simplified model programmed for use on a pocket calculator or slide rule should be adequate, provided the proper weather inputs are available.

Because FLIR design and performance are so strongly dependent upon atmospheric conditions, a knowledge of meteorological conditions is necessary on a number of bases. First, world-wide weather statistics in which data are averaged over all months and many years are needed as inputs to the model to permit it to serve its functions in sensor selection/development/production decision making and as a design tool. Second, weather statistics for a wide variety of areas on a month-by-month basis but

averaged over many years are needed to extrapolate the results of sensor evaluations and to determine where and when the various sensors should be deployed. Third, local weather reports and forecasts are needed for mission planning.

IV. DESCRIPTION OF A FLIR PERFORMANCE MODEL

In FLIR performance modeling, four factors are generally considered: (1) the emission of radiant power from the target, (2) the transmission of that radiation through the atmosphere, (3) the interception of a small fraction of that radiant power and the conversion of its signal information into a visual image, and (4) the viewing and interpretation of the image by an observer. I plan to give you only a synopsis of the processes involved in FLIR performance modeling with emphasis on the effects of weather. Much more complete treatments of these processes are given in reference (a) through (h).

In this discussion we will assume that the targets and backgrounds of interest behave in blackbody radiators; that is, they radiate with 100% efficiency. Figure 1 shows the spectral distribution of radiation emitted by a blackbody at temperatures of 10°, 15°, and 20°C. We see that the peaks occur at a wavelength of about 10 micrometers. As mentioned before, there are atmospheric transmission windows in the intervals from 8 to 13 micrometers and from 3 to 5.5 micrometers. The greater amount of power, by far falls within the longer wavelength interval and, with current technology, this is the better band. For the remainder of this presentation we shall confine our attention to the band running from 8.0 to 12.5 micrometers. Now in most cases we are not particularly interested in the absolute temperatures of targets but rather in differences of temperature among the various objects in the scene. Suppose, for example, that the hull temperature of a ship is 20°C and the background (water) temperature is 15°C. The radiation that would convey information about the ship to the observer is that represented by the area between the 15° and 20° curves of figure 1. To gain an appreciation of the spectral distribution of such differences in radiancy, we can take the first derivative of the 15°C curve with respect to temperature and obtain the curve shown in figure 2. This curve provides a better indication of the spectral band in which our FLIR should operate compared to those in figure 1. Note that the peak has shifted to about 8.5 micrometers.

The amount of information-carrying radiation that is

intercepted by our FLIR receiver also depends upon the size of the target. Figure 3 shows how the effective projected area of a destroyer varies as a function of range from a FLIR-equipped aircraft for various altitudes: p and two target aspect angles. Note that for p = 300 ft., the effective area decreases rapidly at a range of about 22 miles as the target disappears over the horizon.

The second factor in our FLIR performance model is atmospheric transmission. Losses occur because of molecular absorption by gases such as ozone, carbon dioxide and water vapor, and because of scattering and absorption by particulates such as water droplets in fog and haze. Here we shall not consider as a separate parameter scattering by the small droplets associated with haze, but rather assume a fixed scattering loss consistent with "average clear" conditions that is built into the transmission model selected. We shall further assume that if dense fog or thick clouds intervene between the target and the FLIR, then operationally useful detection ranges will not be achievable. The latter situation can be handled statistically on a "go/no-go" basis in terms of cloud-free line-of-sight probabilities.

Now let us consider the molecular absorbers. On the average, atmospheric ozone is concentrated in a layer centered at an altitude of about 79,000 feet. For the relatively low altitudes at which FLIRs are operated typically, it can be deduced from figure 4 that losses due to ozone, even over a 30 mile path, amount to only about 4% over the spectral band of interest. Therefore, losses due to ozone will be neglected.

Carbon dioxide is a strong absorber in certain bands of the infrared spectrum. However, over the 8.0 - to 12.5 micrometer interval, the average loss over a 30 mile path is only 10% as can be inferred from figure 5. Losses due to carbon dioxide absorption will be neglected here also.

The most important and, unfortunately, the most variable atmospheric molecular absorber in the band of interest is water vapor. Its concentration may range from a few tenths of a gram per cubic meter in cold, dry climates to 40 to 50 grams per cubic meter in tropical jungle type climates as figure 6 suggests. To further complicate matters, its concentration varies as a function of altitude as illustrated in figure 7, with the largest concentrations occurring at sea level. To determine the total amount of water vapor within a slant viewing path, we must integrate over that path. Next we try to relate

the amount of water vapor in the path to atmospheric transmission. Figure 8 indicates the great variability in thinking by various students of atmospheric transmission. In figure 8 the water vapor concentration is expressed along the abscissa in terms of the length of the column of water that would result if all the water vapor along the path were to be condensed to liquid. We have some very optimistic people who teach that, even with 50 centimeters of precipitable water in the path, transmission should amount to about 30% whereas the pessimists teach that transmission effectively cuts off with 20 to 25 centimeters of precipitable water in the path. Currently, the most popular atmospheric transmission model for our purpose is the so-called LOWTRAN II model which, compared to others, is relatively pessimistic in the 8.0 - to 12.5 micrometer band, particularly over the longer paths, but relatively optimistic over the shorter paths. In this FLIR performance model, I selected the Altshuler model largely because it seemed like a reasonable compromise between extremes.

The curves in figure 9, which were derived from Altshuler's model, show the transmission of infrared radiation through water vapor as a function of wavelength for various amounts of water vapor, W, in the path. Now, if each of these curves is multiplied point-by-point by the derivative of radiancy curve of figure 2, we obtain the set of "transmission" curves shown in figure 10 which are spectrally weighted to match the anticipated signal radiation characteristics. Next, the area under each of these curves is integrated, and the integrals plotted as a function of the amount of water vapor in the path to obtain the single curve of figure 11. This curve was then redrawn as figure 12 to show how apparent target-to-background temperature difference varies as a function of the amount of water vapor in the target-to-sensor path. Now if we apply figure 12 to the case of a ship that differs in temperature from its background by, say, 5°C and if it is viewed over a path that contains perhaps 30 centimeters of precipitable water, its apparent temperature difference will be reduced to about 10% of its actual value or to 0.5°C.

Next, to relate FLIR laboratory performance to the world of targets, we invoke a concept known as MRT (minimum resolvable temperature difference) which recognizes that the FLIR observer's ability to resolve target details depends upon both the sizes of the target features and the amounts by which they differ in apparent temperature from their surroundings. MRT can be measured in laboratory experiments or calculated from FLIR design

parameters such as the number, size and material of its detector elements, and the characteristics of the optical system. Figure 13 illustrates a set of test patterns that is viewed by a FLIR undergoing an MRT test. The black bars are raised in temperature by some small amount relative to their background (also black) until the observer is able to discern/resolve the largest bars in the pattern. Then the bar-to-background temperature difference is increased gradually until each of the remaining sets of smaller and smaller bars can be resolved. The minimum temperature difference for which each set of bars can be barely resolved is then plotted as a function of the angle subtended by the narrow diminsion of the bars to yield an MRT curve. (In practice, it is generally the "angular frequency" of each set of bars that is plotted as the abscissa rather than the angle subtended. "Angular frequency" is taken as the reciprocal of the angle subtended by a pair of adjacent warm and cool bars.) A representative MRT curve is shown in figure 14.

The next task is to develop criteria for determining the quantity of information required by a FLIR observer to enable him to perform taks such as classifying and identifying ships. "Classification" is taken here as the act of distinguishing whether a given ship is a commerical ship or a warship; "identification" is the act of distinguishing whether a given class of warship is a United States or a Soviet vessel. Figures 15 through 20 illustrate the process used for developing the criteria. It has been concluded that, for reasonable populations of potential targets, between 60 and 70 resolvable elements (pixels) falling on the target is adequate for classification and 400 pixels is adequate for identification.

The foregoing considerations enable us to determine the levels of detail that our FLIR must resolve if the required task is to be performed. This, in turn, can be related through the MRT of the FLIR to the size, range, temperature difference and orientation of the target ship and the concentration of water vapor in the atmosphere. All of these variables have been interrelated by a set of equations and inequalities shown in figure 21, which summarizes our model. By exercising this model for the assumed representative case, described in figure 22, we can obtain curves showing the ranges at which classification and identification can be performed as a function of target-to-background temperature differences.

V. INPUTS TO THE PERFORMANCE MODEL

The next question is "What are realistic numbers to plug into the model to enable it to yield meaningful answers?" For example, should we assume that the ship-to-background temperature difference is going to be 10 or 10^{o} or 0.1^{o} or what? Such temperature differences are quite variable, depending upon factors such as time of day, sea state, cloud cover, wind direction and the ship's heading relative to the waves. Because water is very opaque in the 8- to 13-micrometer band, the ship may become more difficult to detect if it becomes covered with spray. In reference (h), statistical data on ship-to-background temperature differences averaged over the entire ship and expressed in the form of histograms and cumulative frequencies of occurrence are given. Reference (h) reports that about 50% of the time we can expect temperature differences of $4.7^{o}C$ or more to exist. However, if we wish to operate at the 90% level, we should design our FLIR with the idea that temperature differences of only about $1.3C^{o}$ can be relied upon 90% of the time.

Another area in which statistical information represents an important input to the model is that of atmospheric water vapor concentration. Reference (d) and (e) describe how published weather data were used to generate histograms and cumulative frequency of occurrence curves for given concentrations of water vapor for 21 selected maritime sites throughout the northern hemisphere. These sites are listed and identified in table I. The Naval Weather Service Command publishes a set of documents called "Summary of Synoptic Meteorological Observations" which provides a wealth of data arranged in all sorts of nice tables. Figure 23 is a copy of a page from one of these documents for "Boston" in May. "Table 13" (shown in figure 23) provides temperature and relative humidity data from which absolute humidities can be calculated and expressed in statistical form as shown in figures 24 and 25. Unfortunately, the grid structure of the matrix of "table 13" is rather coarse; that is, it tells us that 16% of the time in "Boston" in May the temperature is between 45^{o} and $49^{o}F$ at the same times as the relative humidity is between 90 and 100%. Figure 26 illustrates how these uncertainities in temperature and relative humidity combine to produce even larger uncertainties (of the order of $\pm$ 11% relative to mean values) in absolute humidity figures based upon them. Nevertheless, the calculations were performed and the results plotted for the selected sites on both monthly and annual bases. As an example, figure 27 provides data for "Port Said" for

the month of June. The dashed lines indicate the extreme values permitted by the data and the solid center line gives the mean values. As a second example, figure 28 shows the data for "San Francisco" on an annual basis.

A composite over the 21 sites on an annual basis was plotted as shown in figure 29. The significance of these data is that if we want to design a FLIR for world-wide use that will not be prevented by high absolute humidity from achieving its performance goals, say 90% of the time, we would have to design it to cope with an absolute humidity of about 23 grams per cubic meter. Figure 30 was plotted from the same data as figure 29 except that the absolute humidity or water vapor concentration is expressed in centimeters of precipitable water per nautical mile.

Typically, FLIRs seem able to see reasonably well through as much as about 20 centimeters of precipitable water in the path. Thus, for a very low absolute humidity of one centimeter per nautical mile (a value which is not exceeded 10% of the time), ranges out to about 20 miles might be expected. However, if we want to work at the 98% cumulative probability level, we must assume absolute humidities of up to five centimeters per nautical mile and ranges of the order of four miles.

VI. CONCLUSIONS

Several conclusions relevant to meteorology and climatology proceed from the foregoing.

First, there is a need for more precise absolute humidity statistics expressed as probability densities (histograms) and as cumulative frequencies of occurrence to serve as inputs to FLIR performance models. To provide precision greater than that of references (d) and (e) we should go into the data bank and calculate absolute humidities from corresponding pairs of simultaneously measured values of temperature and relative humidity rather than working with values averaged over fairly large intervals.

Second, there is a need for including absolute humidity in routine periodic weather reports and forecasts to enable our operating forces to correlate FLIR performance with measurable environmental parameters.

Third, there is a need for cloud-free line-of-sight statistics providing the probabilities of cloud-free paths

from aircraft to the surface as a function of aircraft altitude, viewing angle, geographical location and time of year.

VII. REFERENCES

(a) NAVAIRDEVCEN (C) Tech Memo ADC-AEY-3:PMM/NEM of 16 June 1972, "Signal-to-Noise Ratio, Noise Equivalent Temperature Difference, Index of Performance and Design-Performance Tradeoffs for FLIR Imaging Devices"

(b) NAVAIRDEVCEN Tech Memo NADC-20203:PMM of 19 Oct 1972, "Mathematical Model of FLIR Performance"

(c) NAVAIRDEVCEN Tech Memo NADC-20203:PMM of 12 Dec 1972, "Predictions of FLIR Performance Against Ships"

(d) NAVAIRDEVCEN Tech Memo NADC-20203:GBL/PMM of 28 Dec 1972, "Monthly Absolute Humidity Propabilities for Selected Marine Locations"

(e) NAVAIRDEVCEN Tech Memo NADC-20203:PMM of 24 February 1973, "Annual Absolute Humidity Probabilities for Selected Marine Locations"

(f) NAVAIRDEVCEN (C) Tech Memo NADC-202149:NEM of 13 Mar 1973, "Distributions of Slant Ranges for Successful Releases of Selected Weapons from the A-7E Aircraft"

(g) NAVAIRDEVCEN Tech Memo NADC-202149:NEM of 30 Mar 1973, (rev 25 Sep 1973), "Naval and Merchant Ship Length Distributions"

(h) NAVAIRDEVCEN (C) Tech Memo NADC-20203:NEM/PMM of 16 Sep 1974, "Ship-to-Background Temperature Differences"

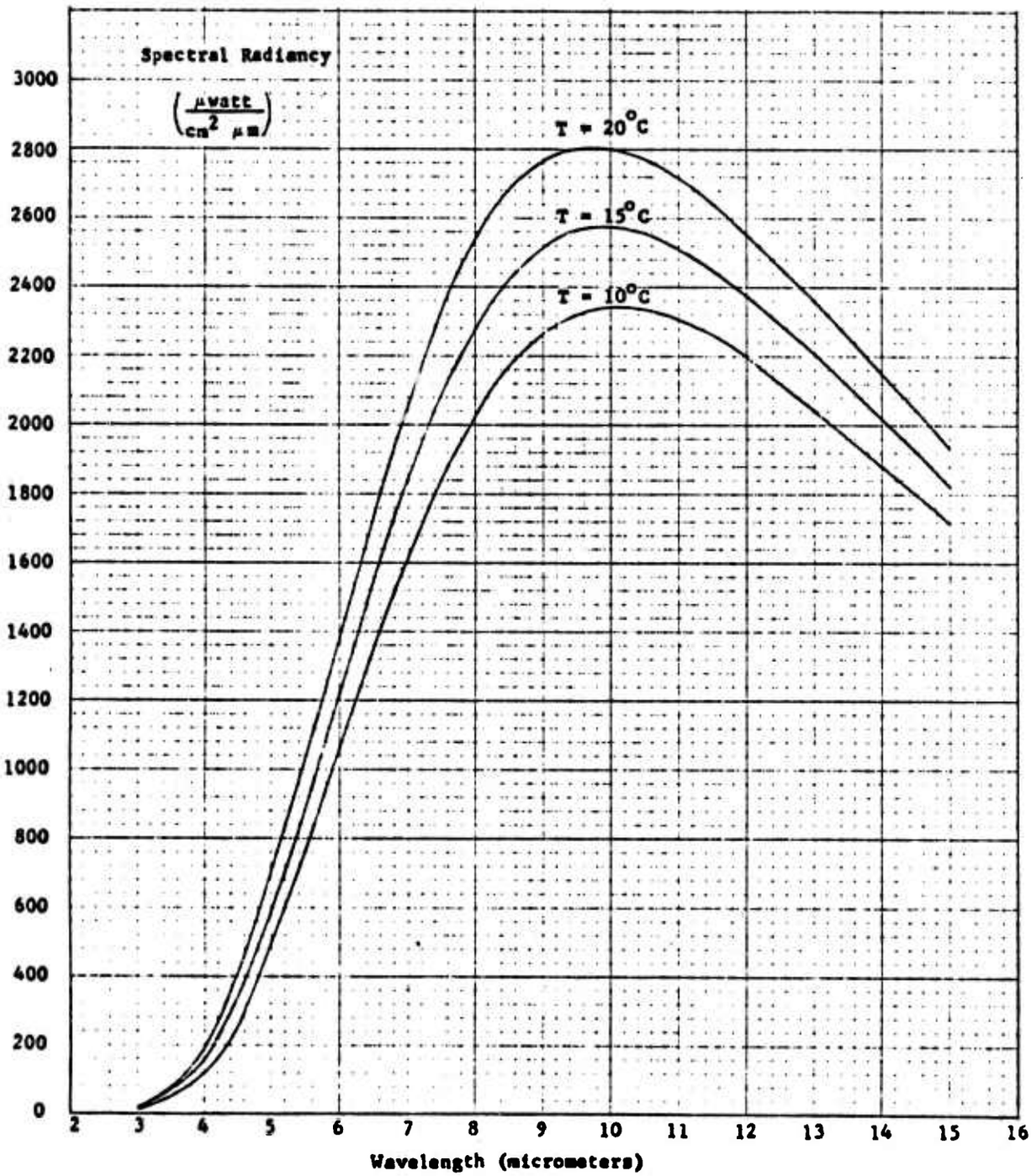

Fig. 1 — Spectral radiancy of a blackbody

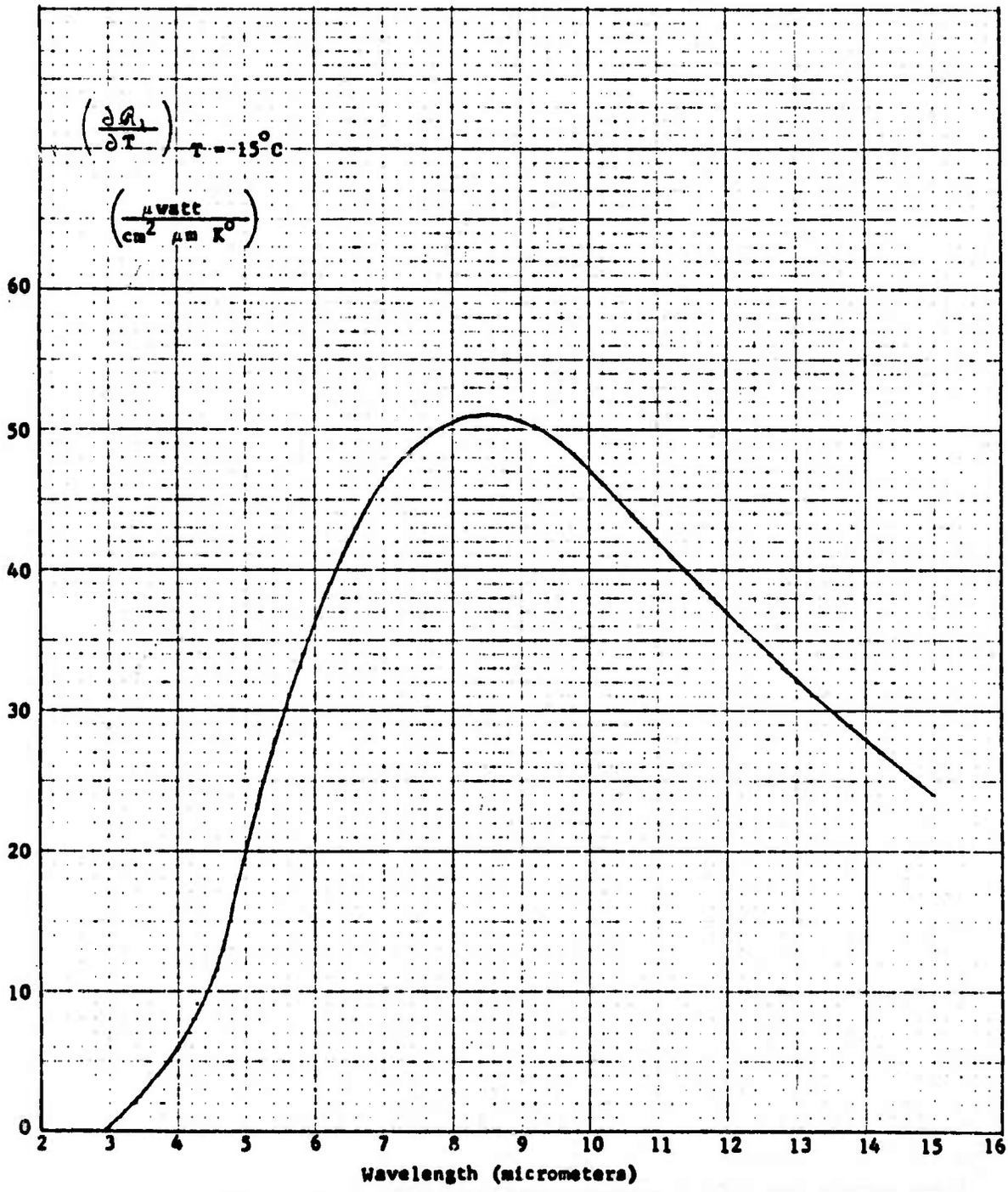

Fig. 2 — First partial derivative of the spectral radiancy of a 15°C blackbody with respect to temperature

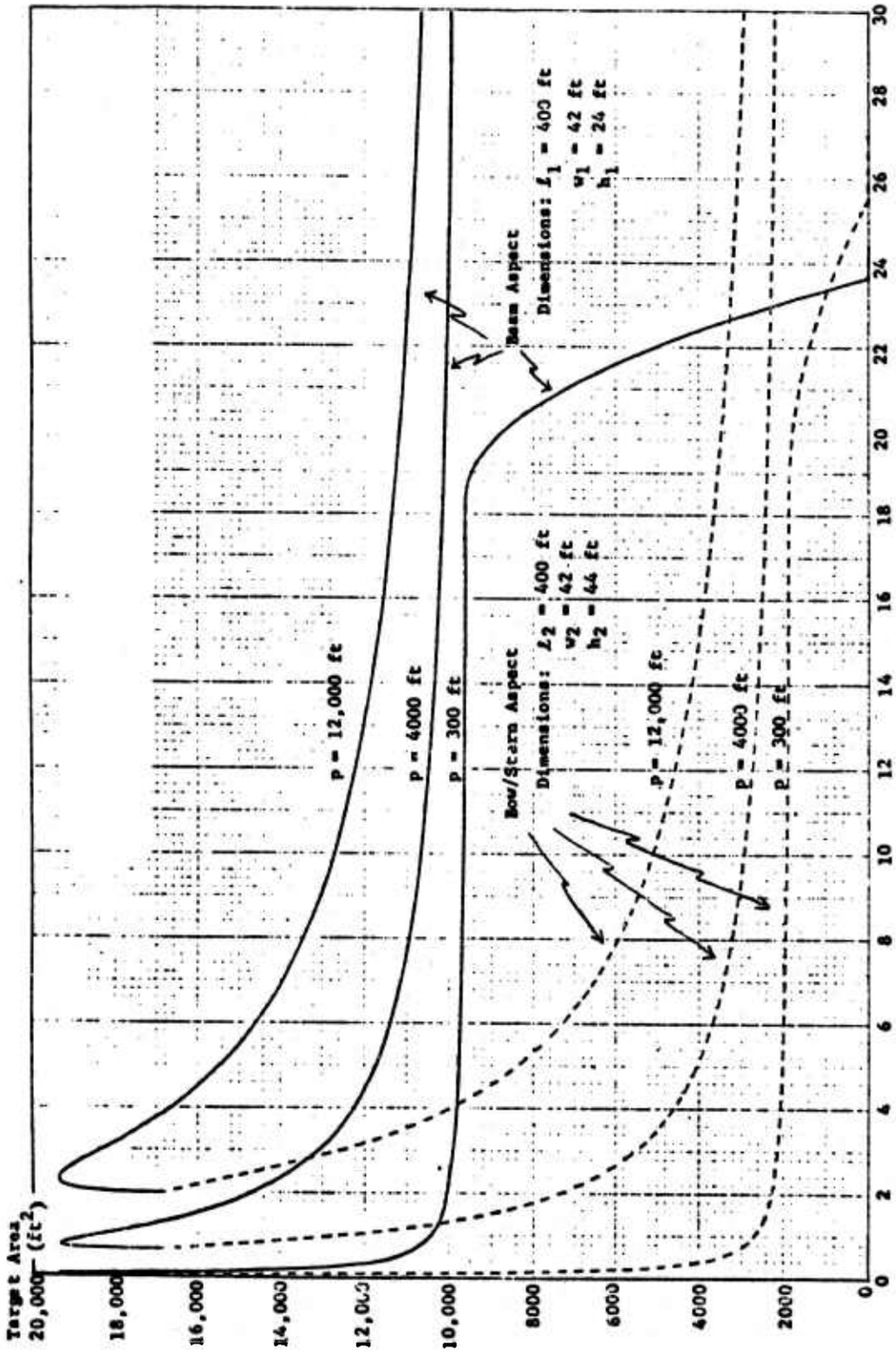

Fig. 3 — Effective projected area of a destroyer as a function of slant range for various sensor altitudes

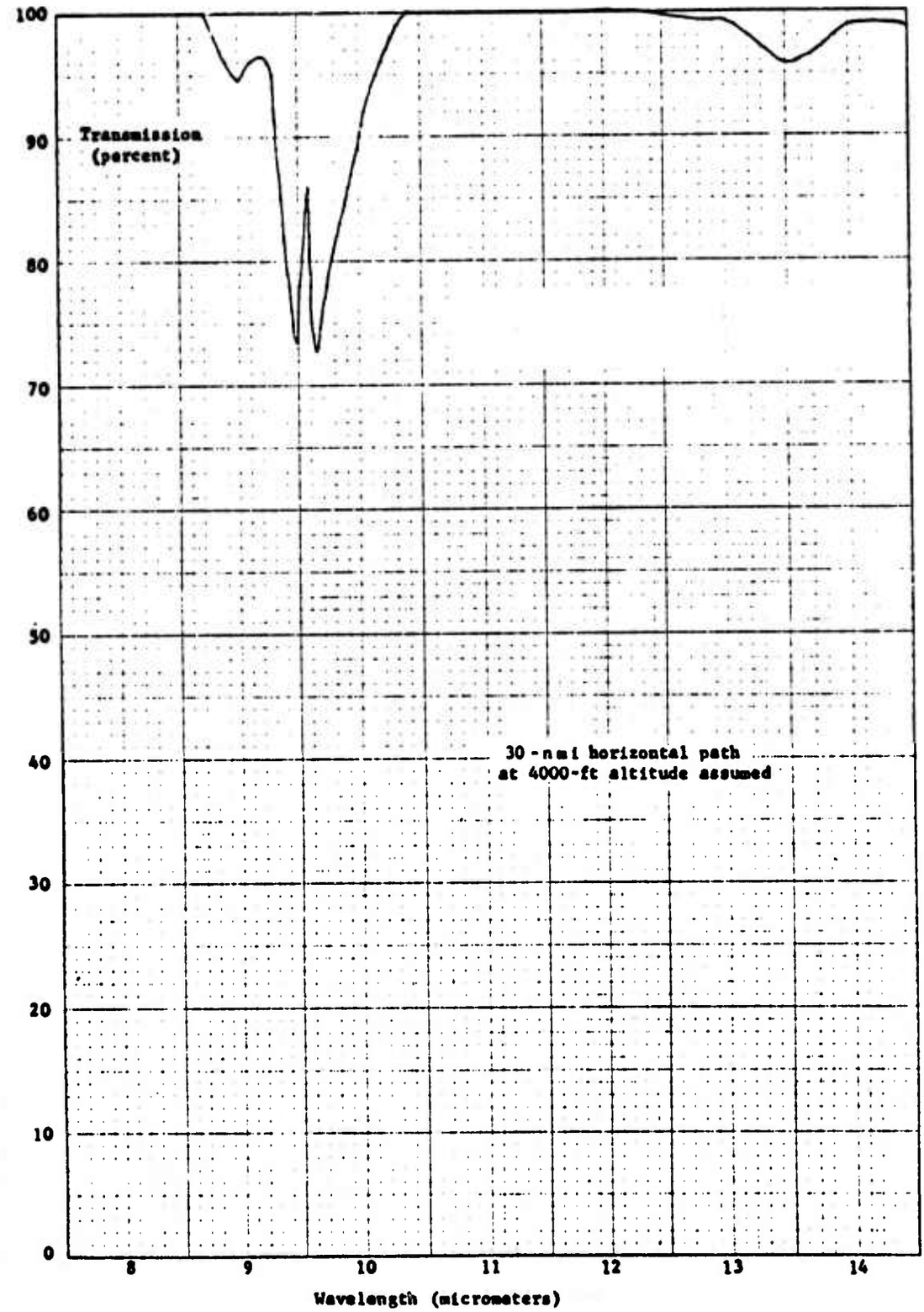

Fig. 4 — Percent spectral transmission of infrared radiation through atmospheric ozone

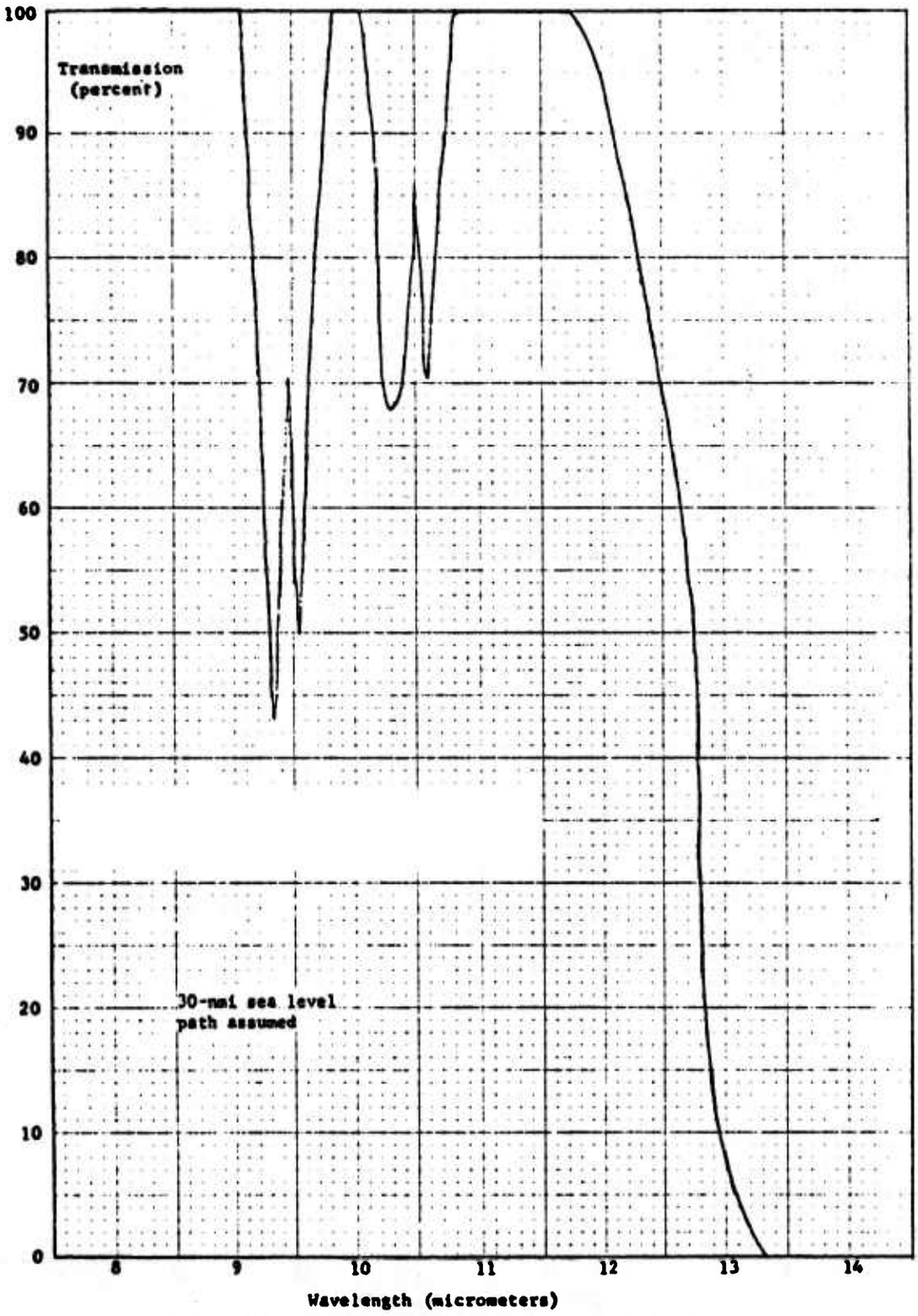

Fig. 5 — Percent spectral transmission of infrared radiation through atmospheric carbon dioxide

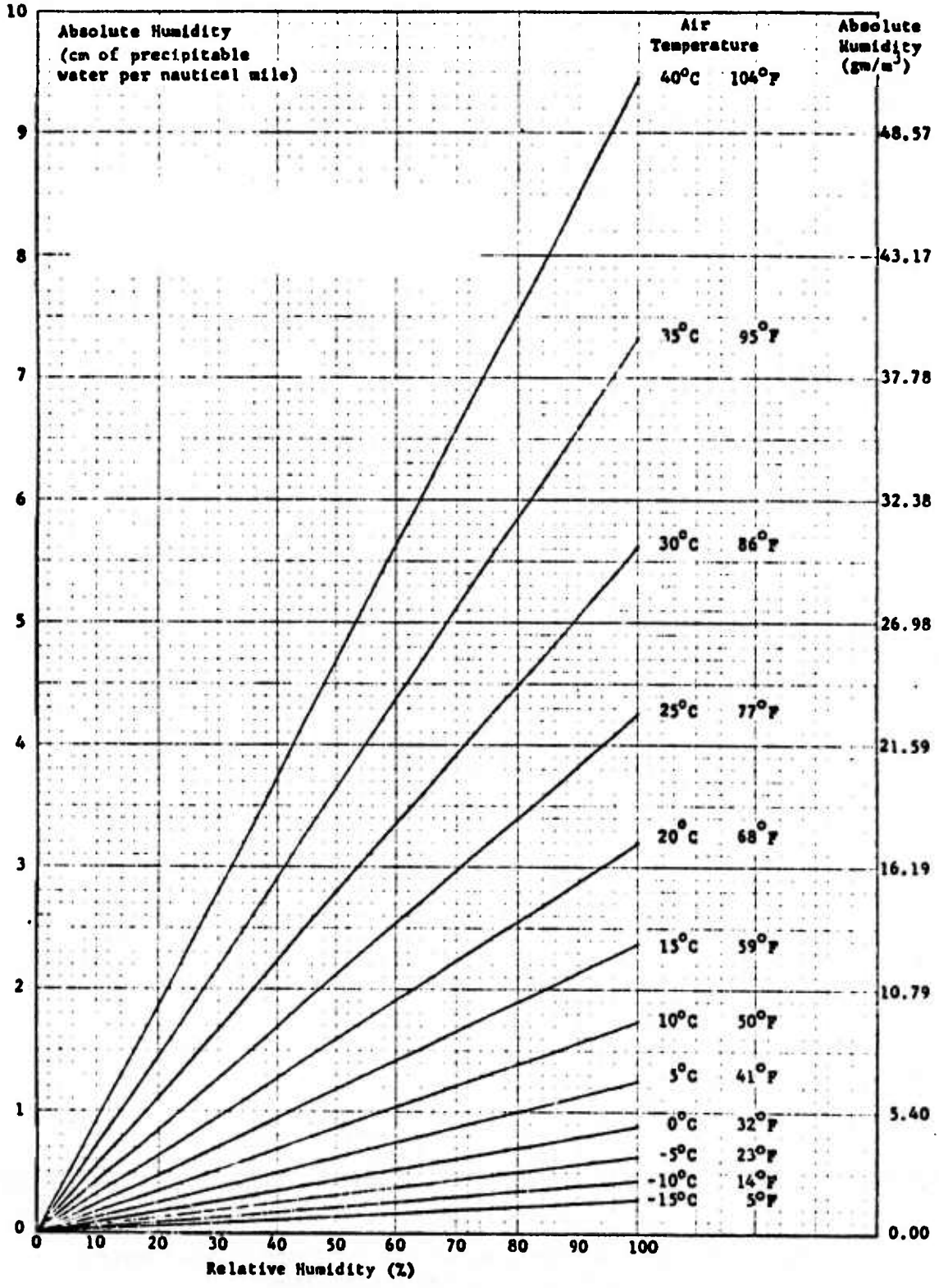

Fig. 6 — Interrelation of absolute humidity, relative humidity and air temperature

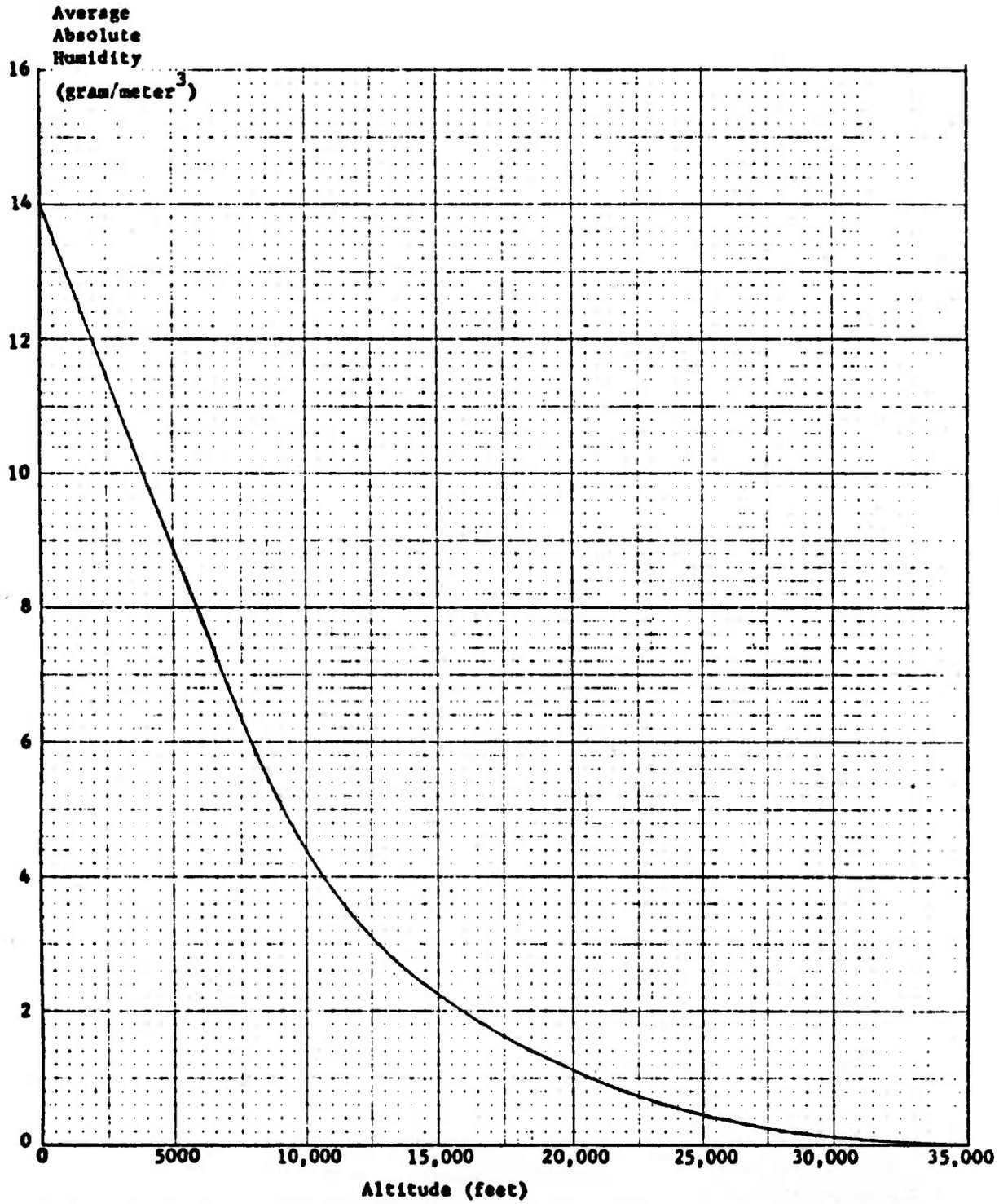

Fig. 7 — Average atmospheric water vapor concentration as a function of altitude for eastern United States

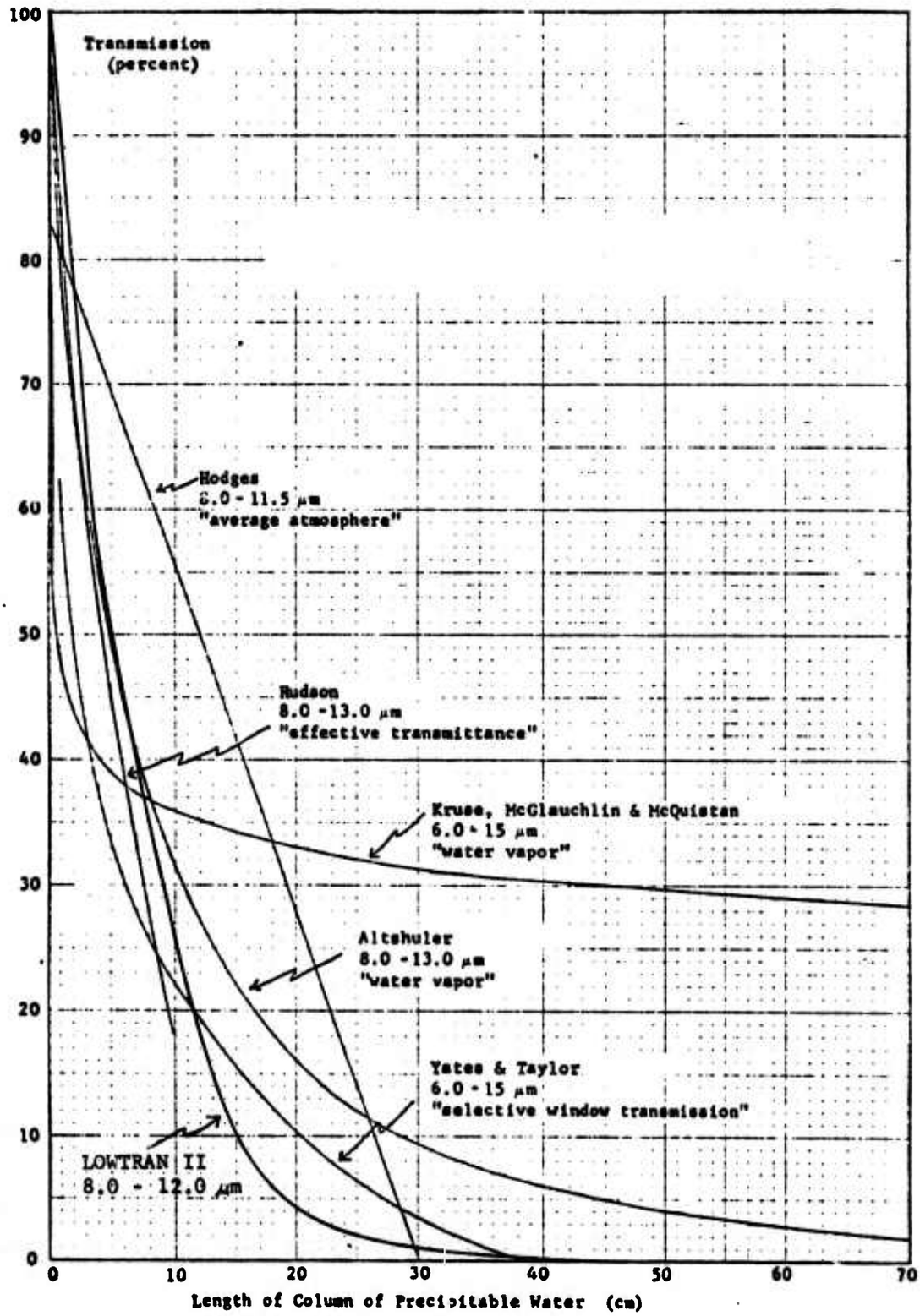

Fig. 8 — Transmission of infrared radiation through the atmosphere along a horizontal sea-level path

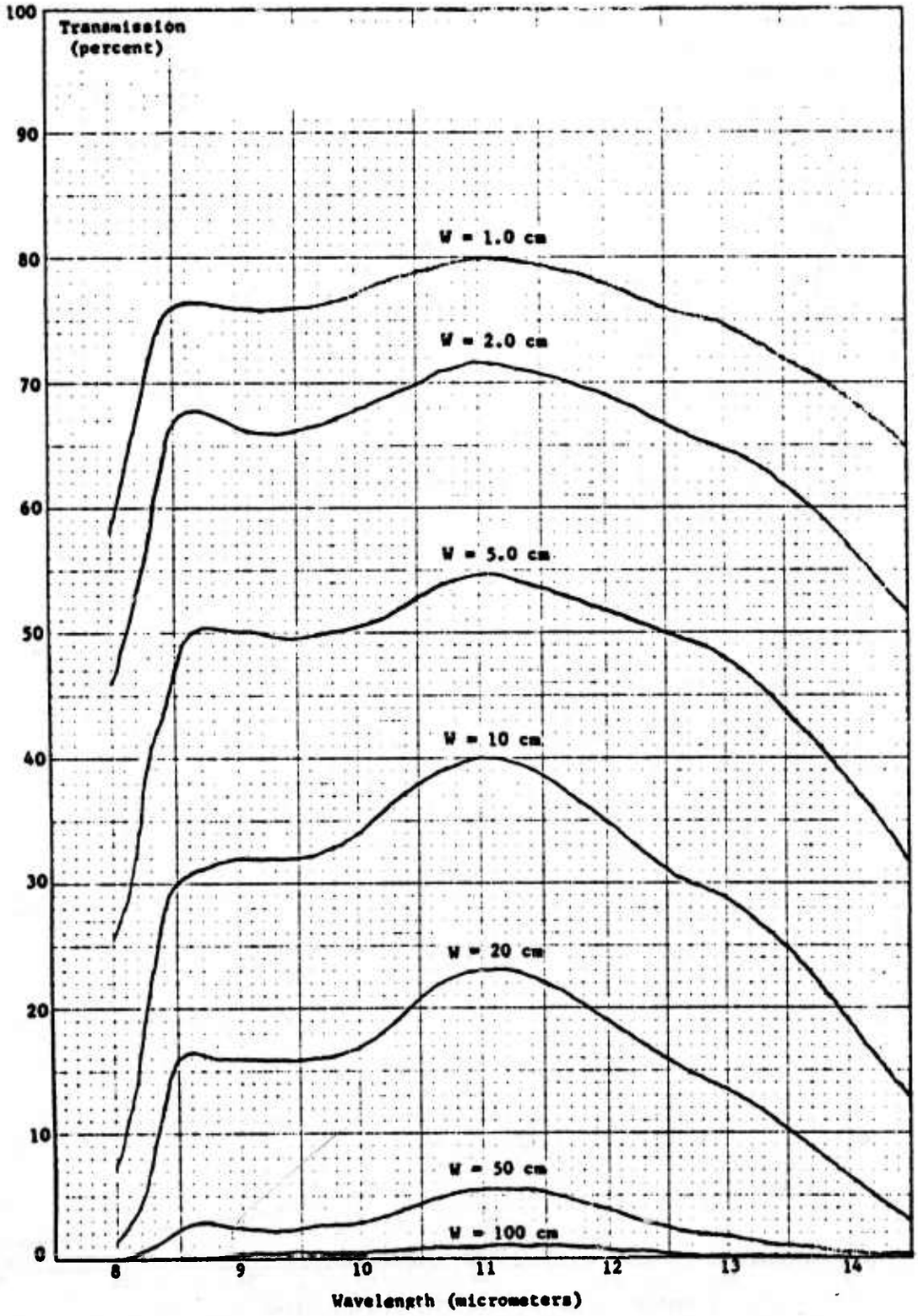

Fig. 9 — Percent spectral transmission of infrared radiation through precipitable water vapor at sea level

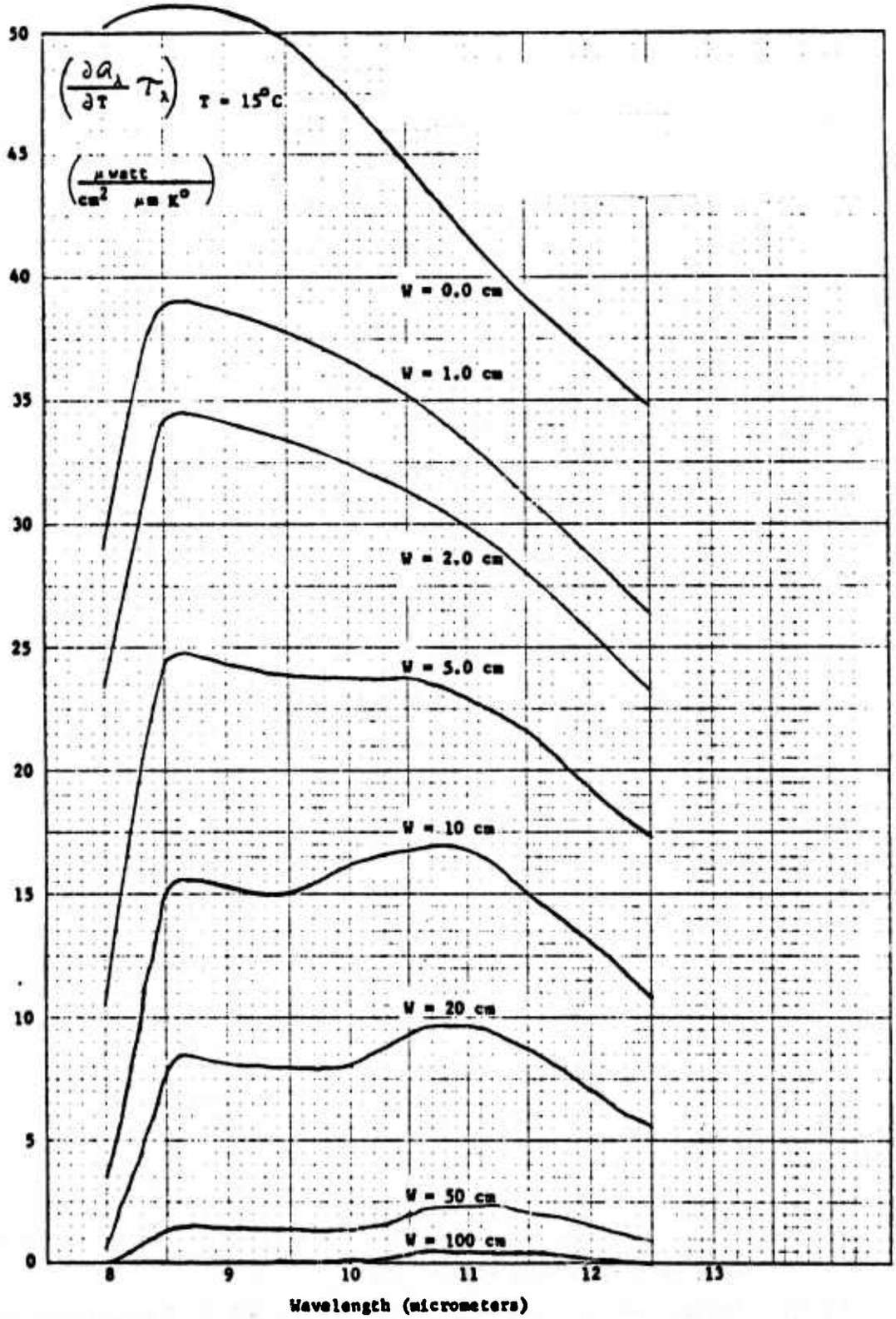

Fig. 10 — First partial derivative of the spectral radiancy of a 15°C blackbody with respect to temperature modified by transmission through precipitable water vapor at sea level

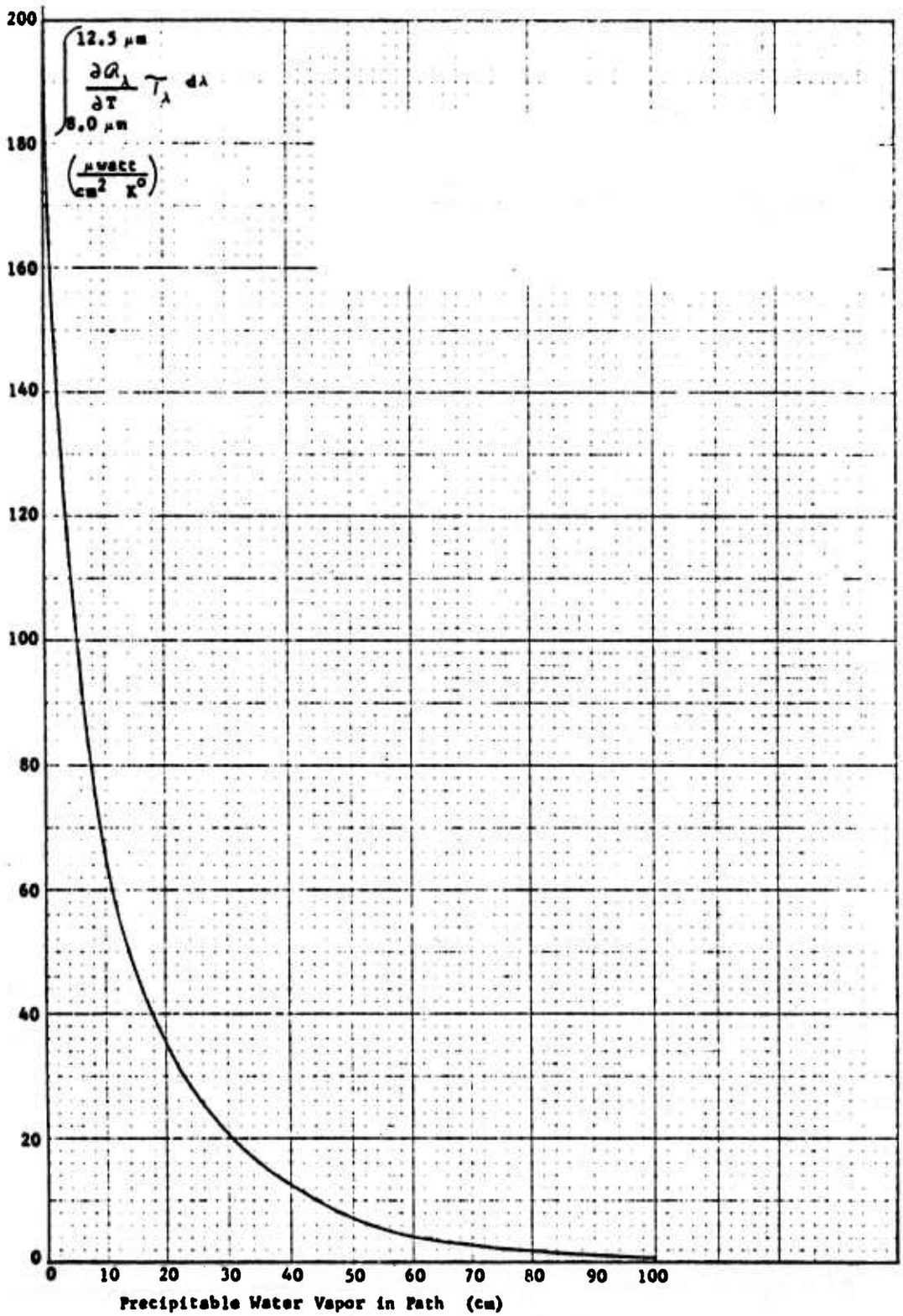

Fig. 11 — Integral over the wavelength interval 8.0 μm $\leqslant \lambda \leqslant$ 12.5 μm of the first partial derivative of the spectral radiancy of a 15°C blackbody with respect to temperature modified by transmission through atmospheric precipitable water vapor at sea level

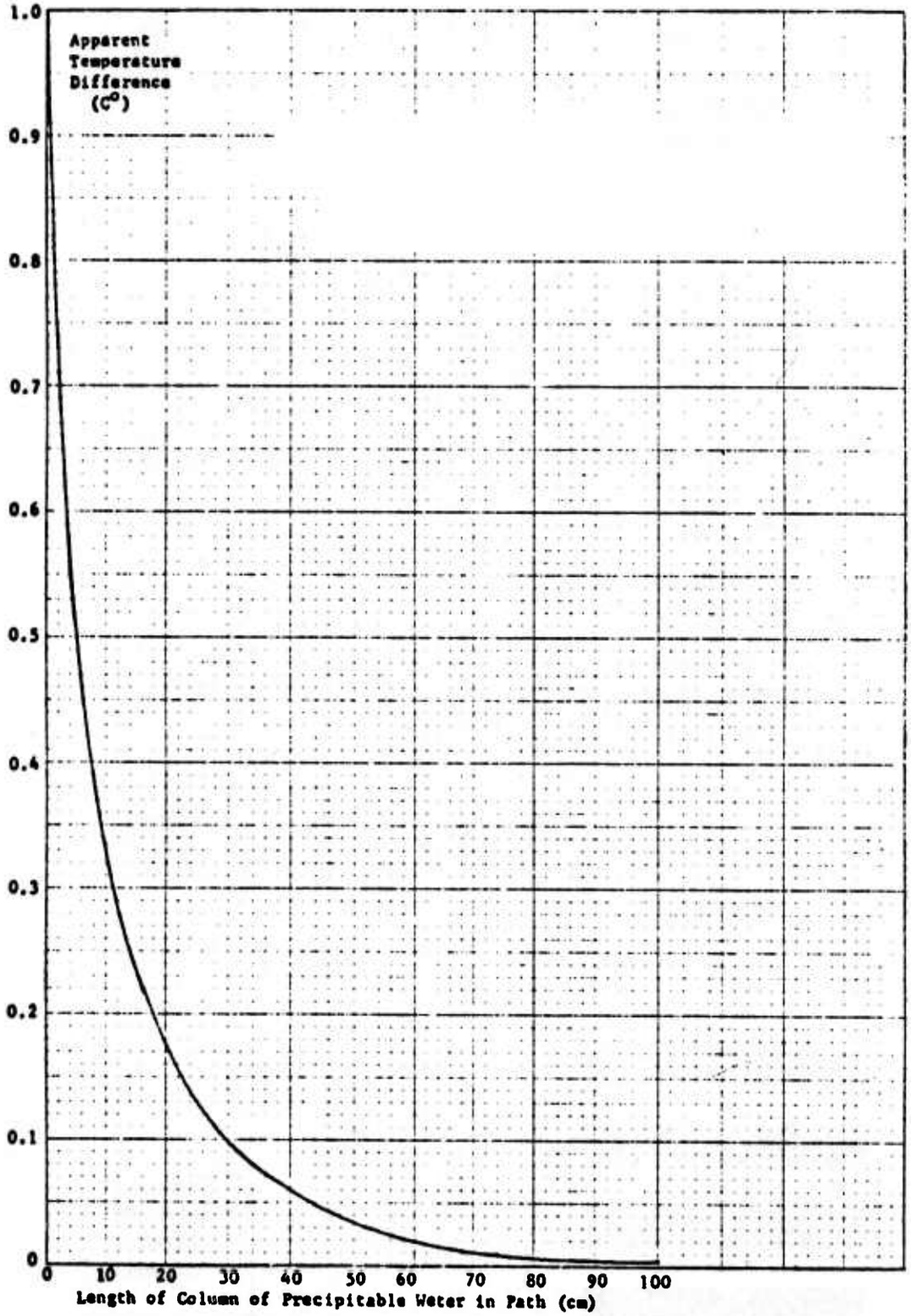

Fig. 12 — Apparent target-to-background temperature difference for an extended area blackbody differing in temperature from its background by 1.0°C as a function of the amount of water vapor in the path between target and sensor

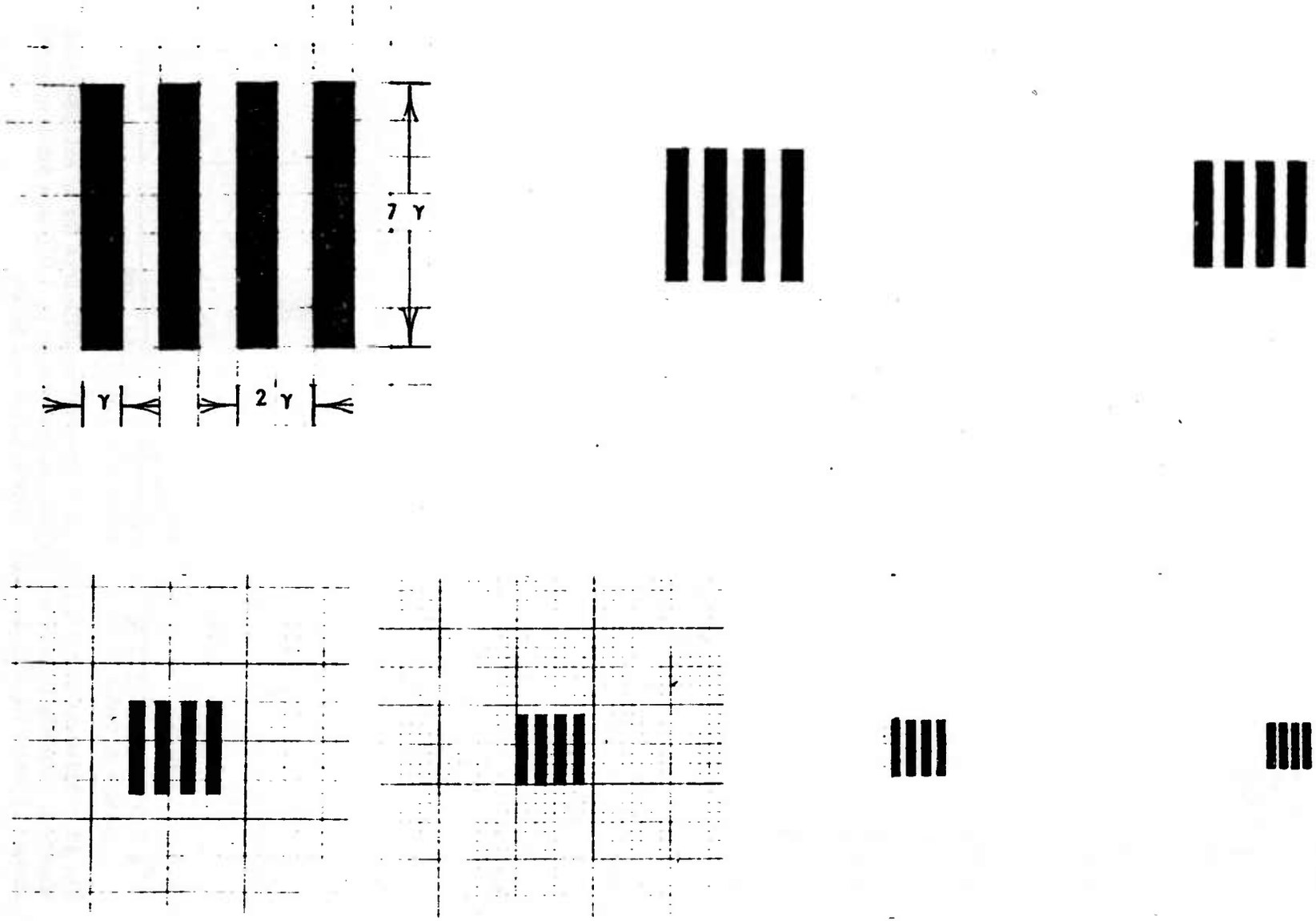

Fig. 13 — Geometry of four-bar target array used in MRT determination

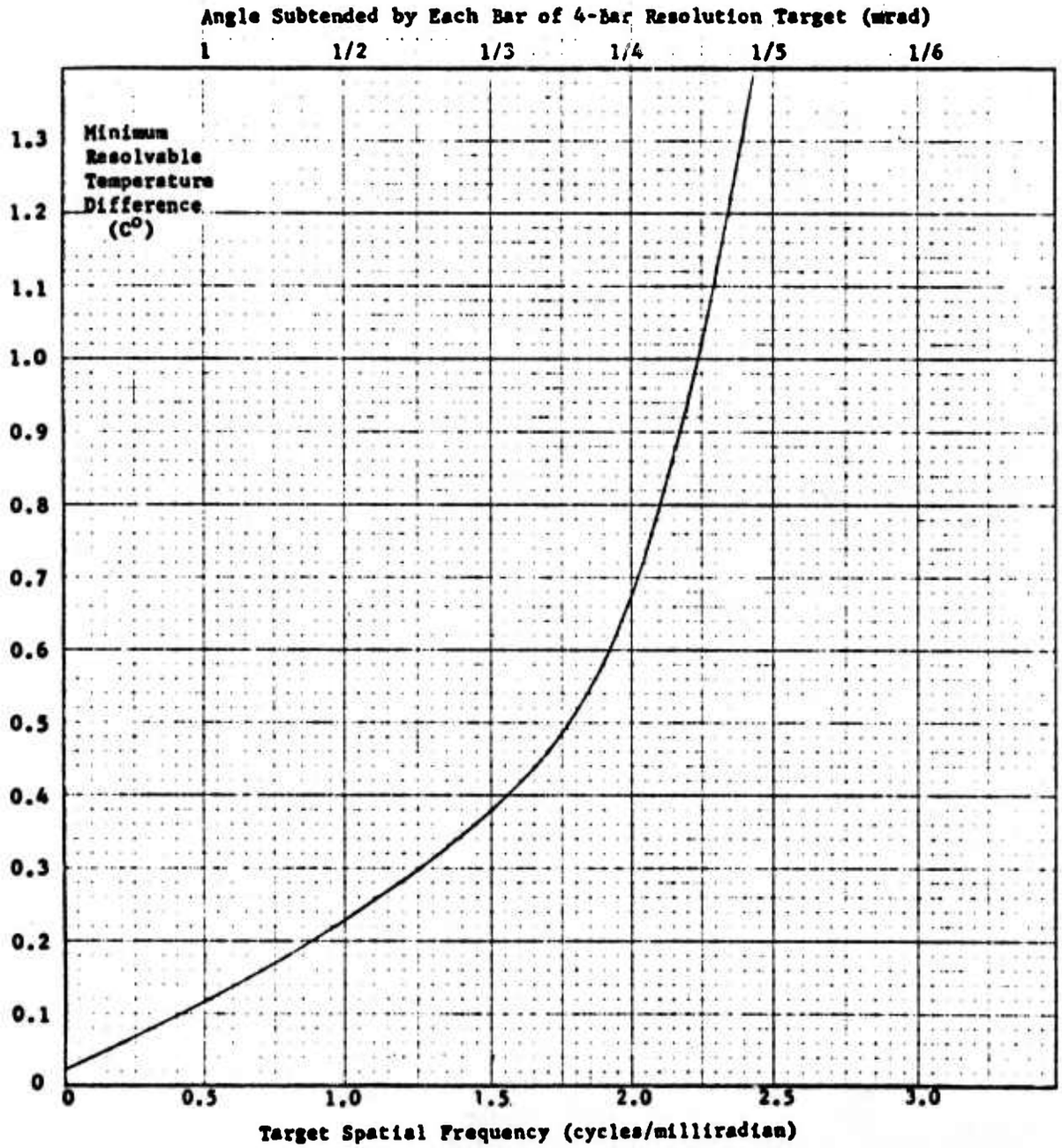

Fig. 14 — Representative MRT curve for a FLIR of 0.25-mrad nominal resolution and 0.25°C noise equivalent temperature difference

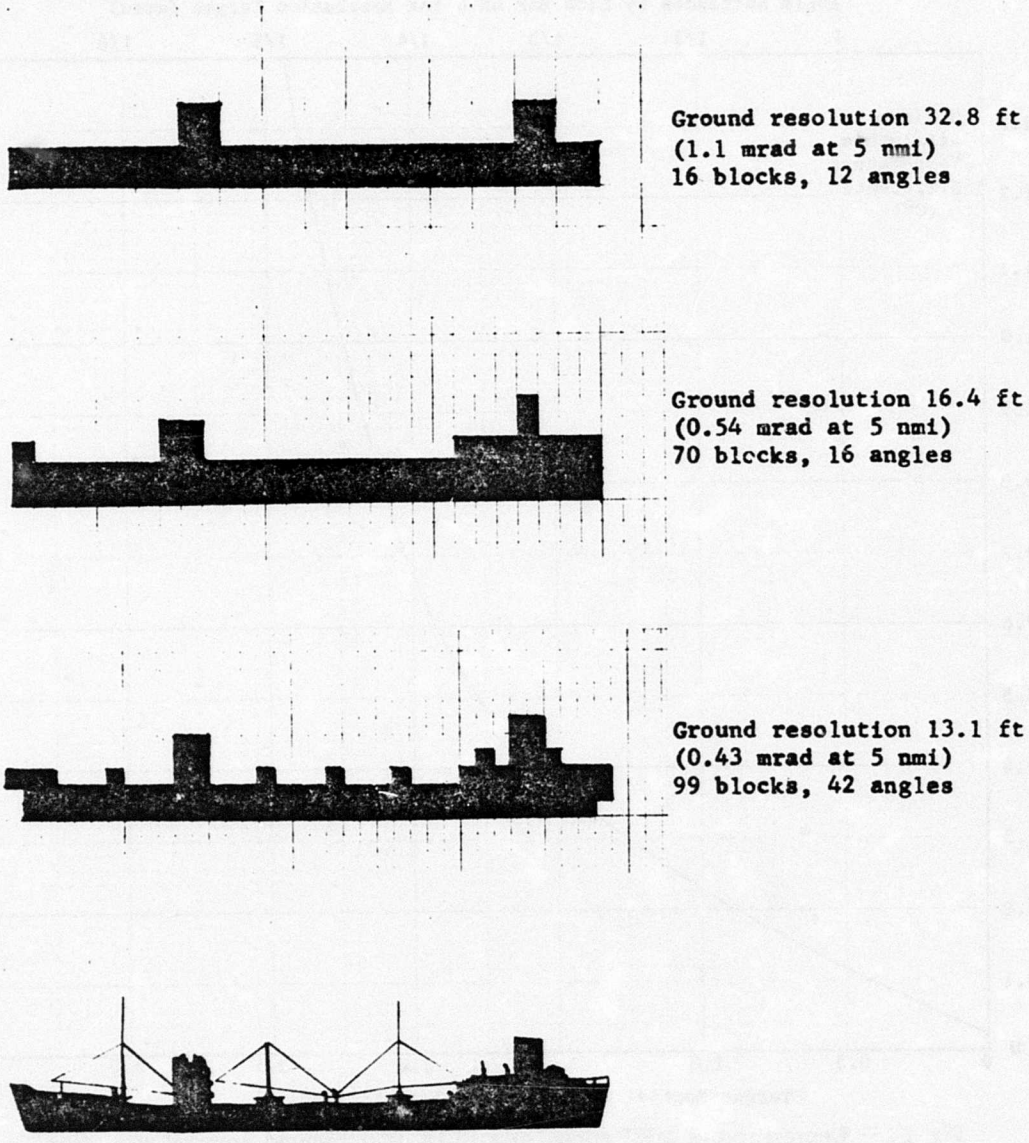

Fig. 15 — Block-type and graphic profile silhouettes of a freighter (Hera, Majoy). Scale 131 ft/in.

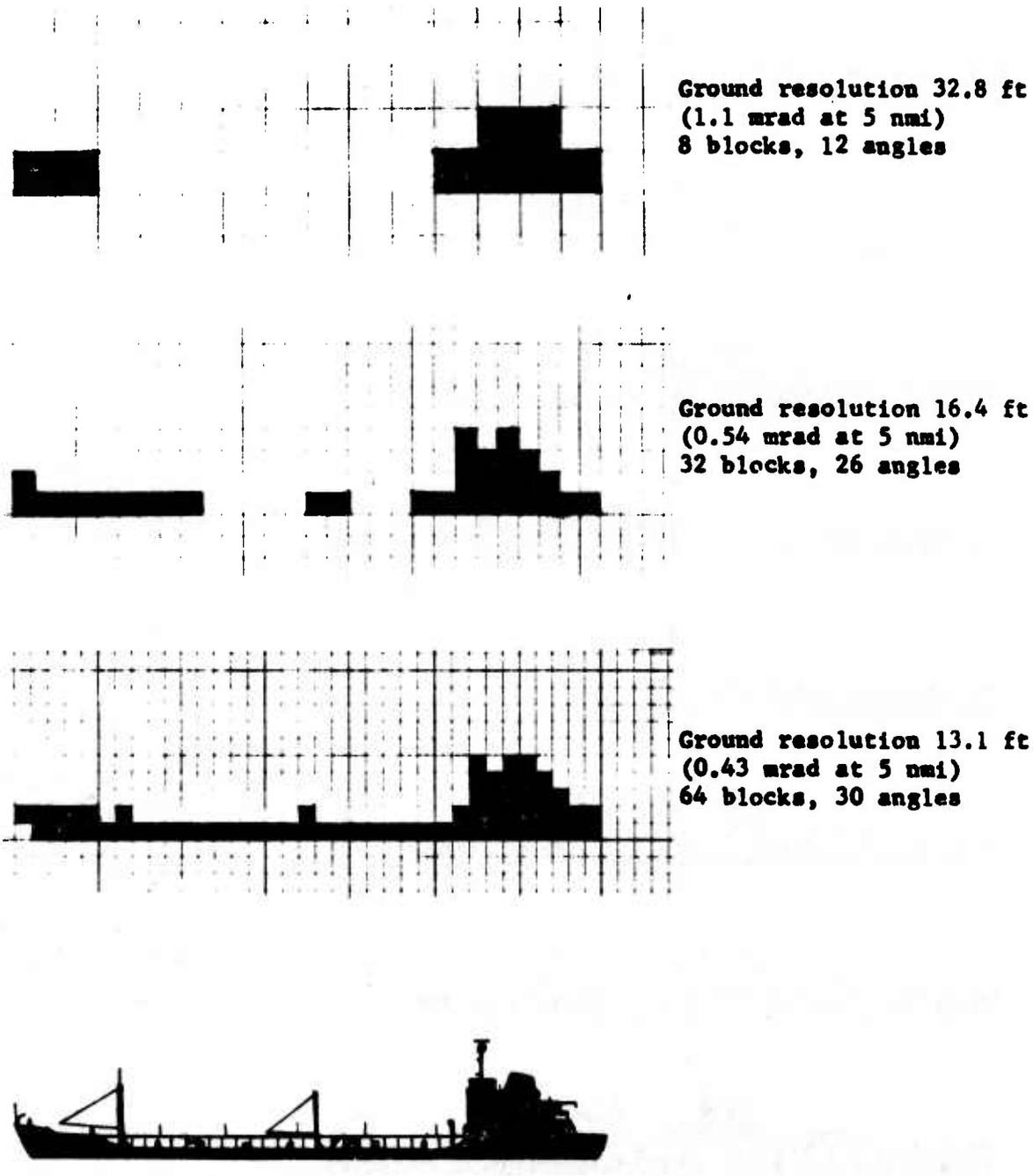

Fig. 16 — Block-type and graphic profile silhouettes of a small tanker (Taquipe). Scale 131 ft/in.

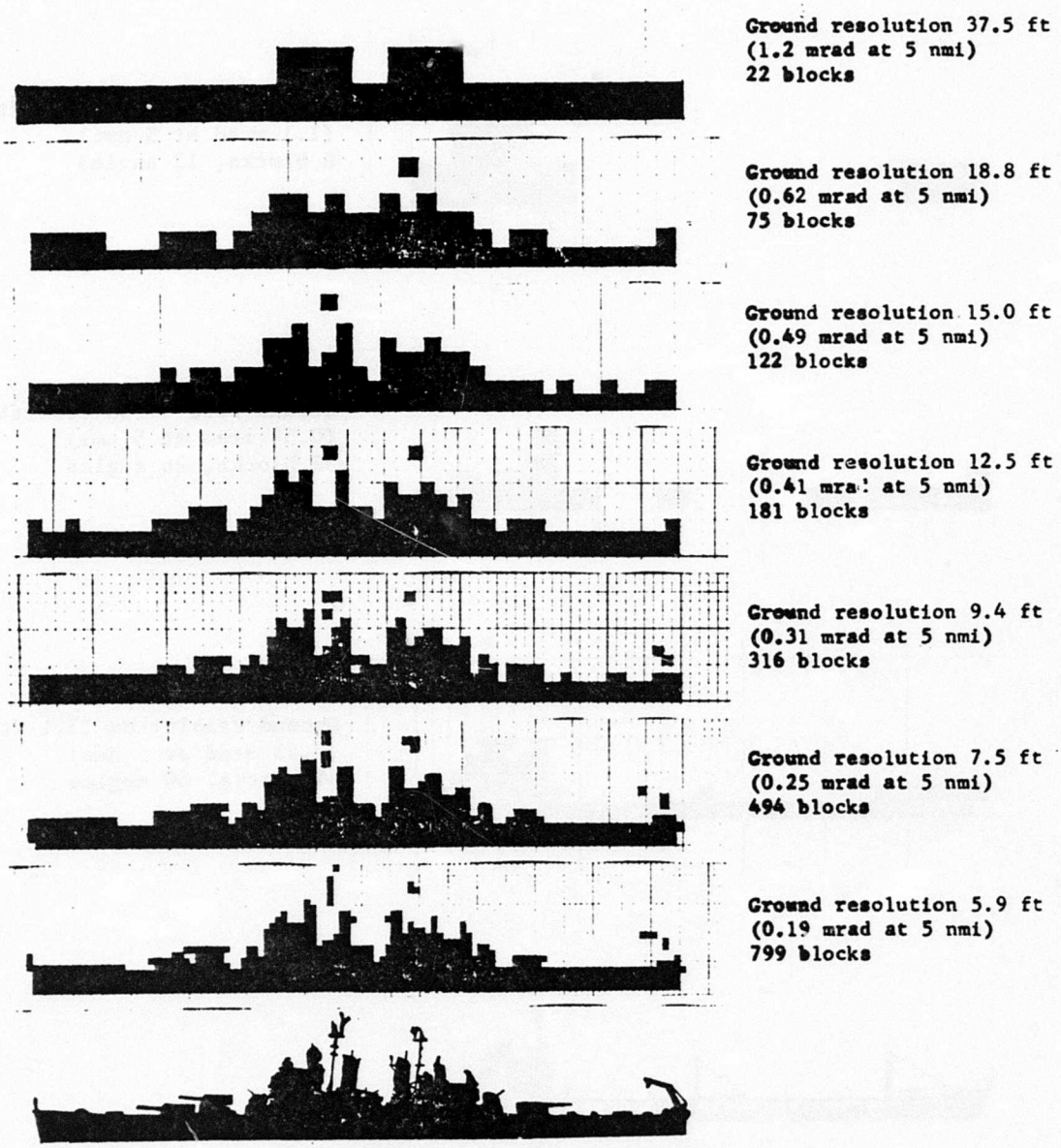

Fig. 17 — Block-type and graphic profile silhouettes of a Baltimore class heavy cruiser. Scale 150 ft/in.

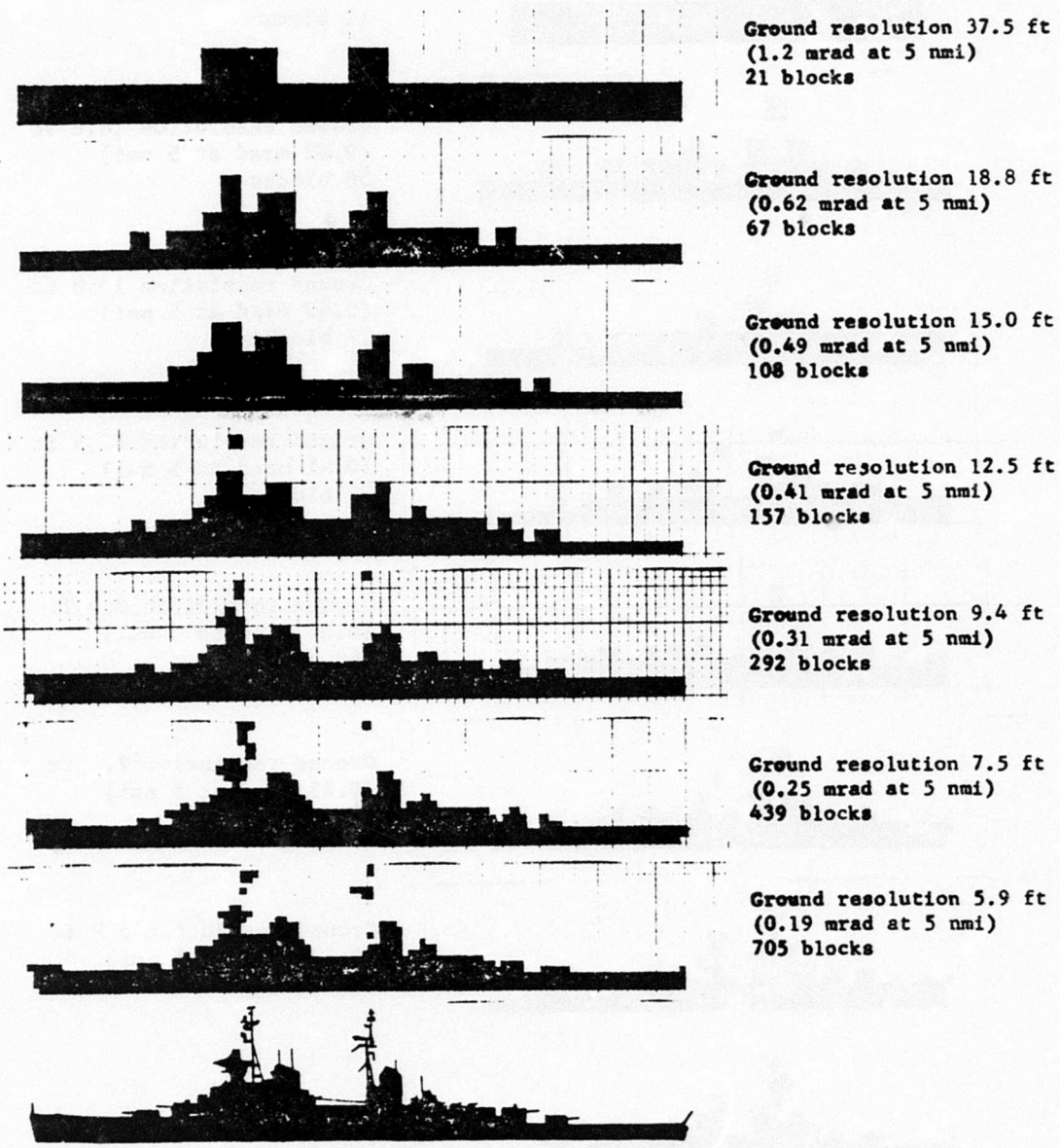

Fig. 18 — Block-type and graphic profile silhouettes of a Sverdlov class cruiser. Scale 150 ft/in.

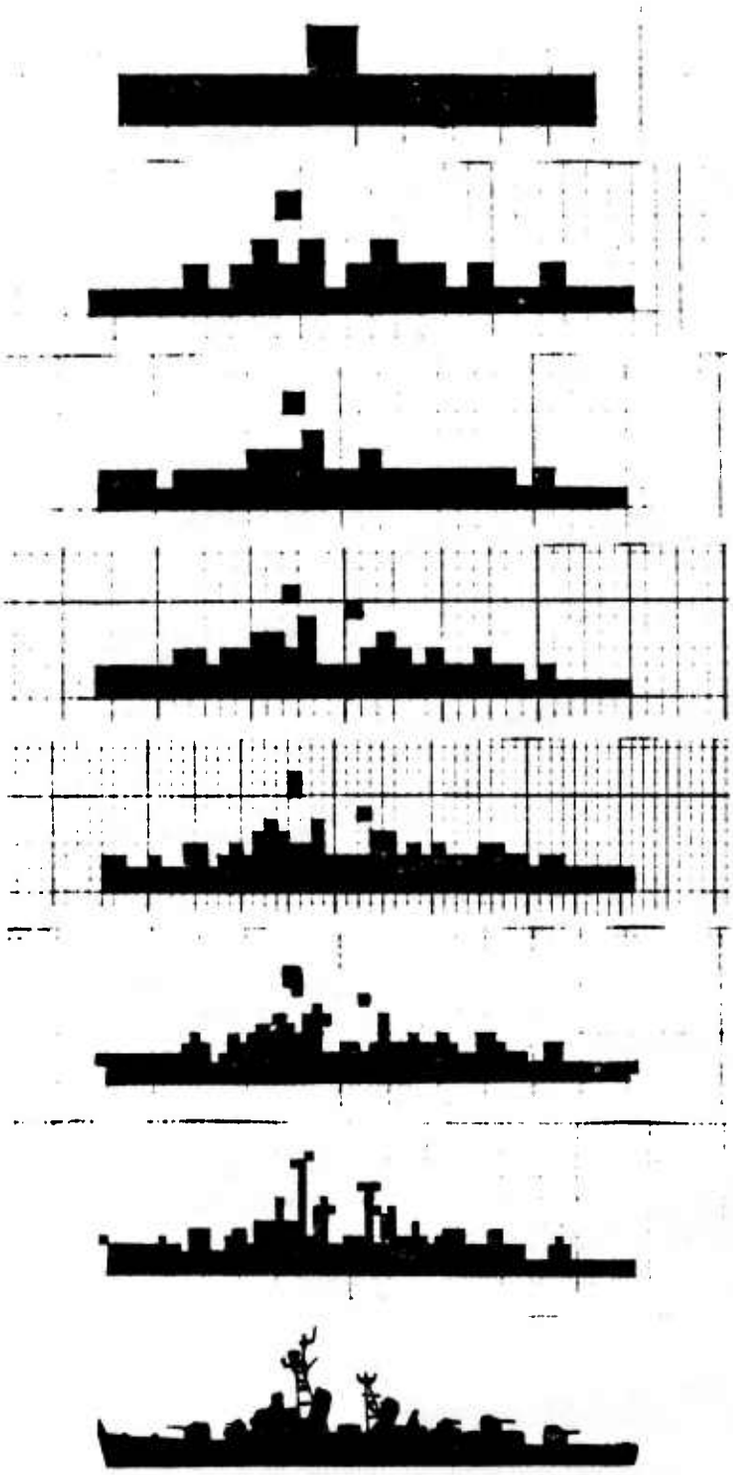

Fig. 19 — Block-type and graphic profile silhouettes of a Forrest Sherman class destroyer. Scale 150 ft/in.

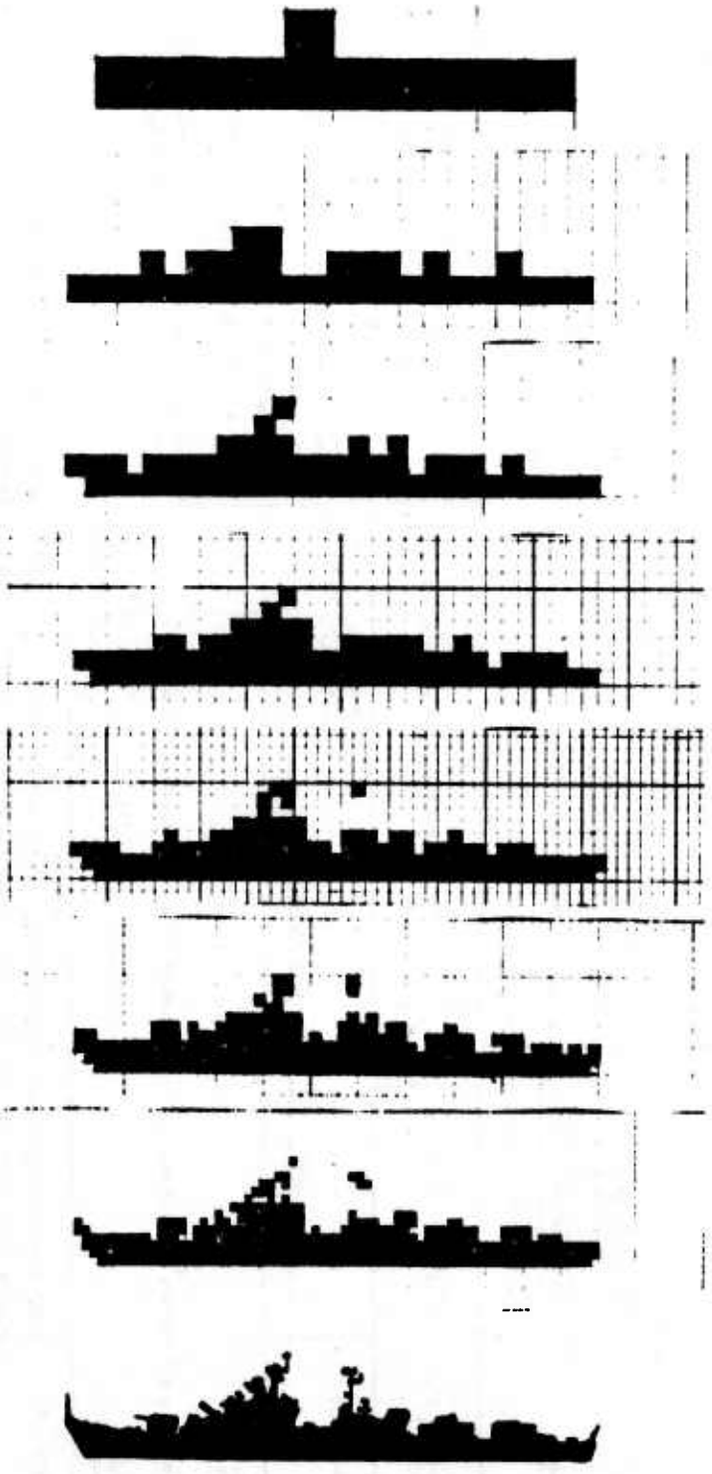

Ground resolution 37.5 ft
(1.2 mrad at 5 nmi)
11 blocks

Ground resolution 18.8 ft
(0.62 mrad at 5 nmi)
34 blocks

Ground resolution 15.0 ft
(0.49 mrad at 5 nmi)
56 blocks

Ground resolution 12.5 ft
(0.41 mrad at 5 nmi)
84 blocks

Ground resolution 9.4 ft
(0.31 mrad at 5 nmi)
146 blocks

Ground resolution 7.5 ft
(0.25 mrad at 5 nmi)
227 blocks

Ground resolution 5.9 ft
(0.19 mrad at 5 nmi)
367 blocks

Fig. 20 — Block-type and graphic profile silhouettes of a Kotlin class destroyer. Scale 150 ft/in.

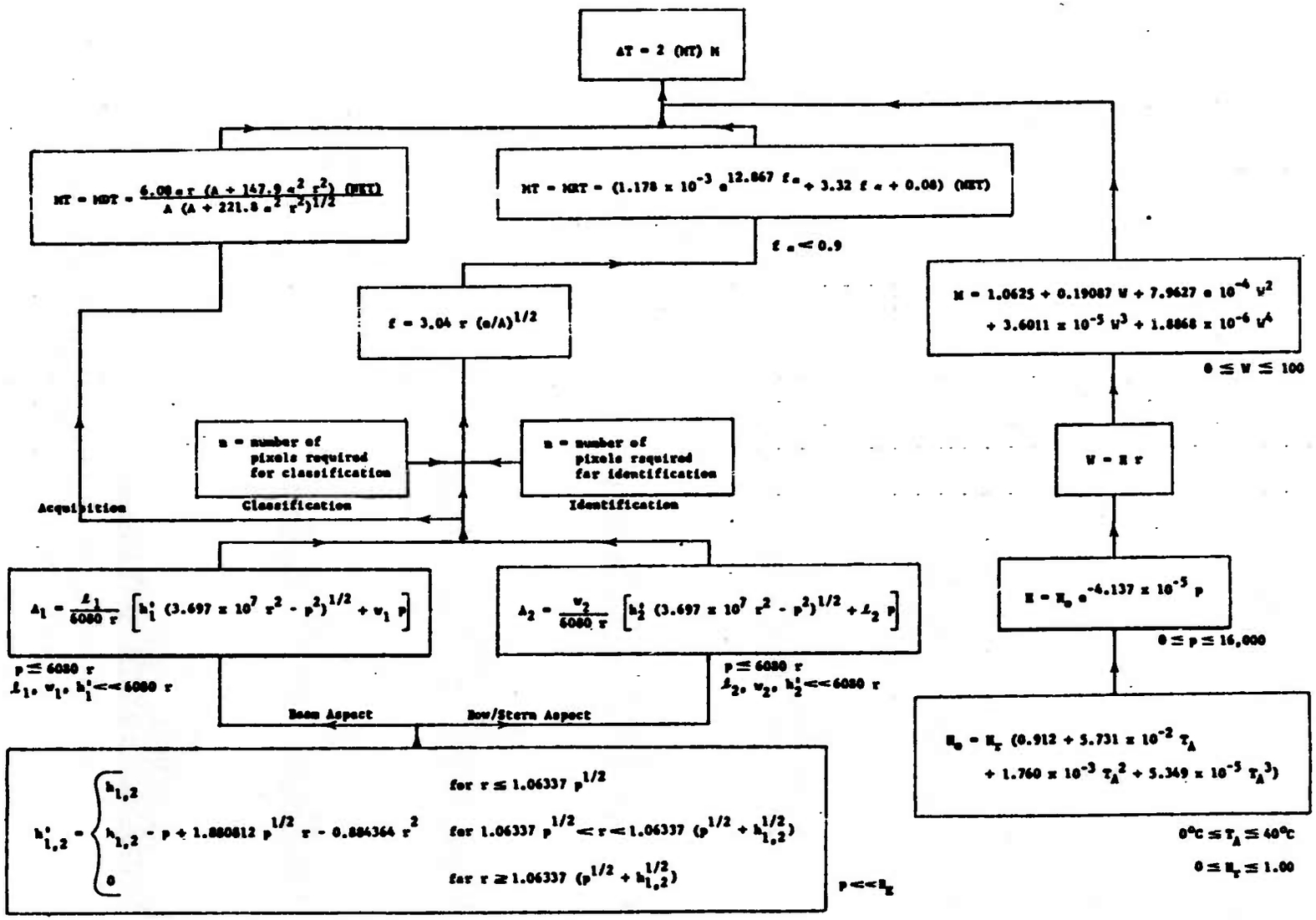

Fig. 21 — Target-to-background temperature differences required to permit acquisition, classification and identification of ships by airborne passive FLIR (forward looking infrared) imaging devices

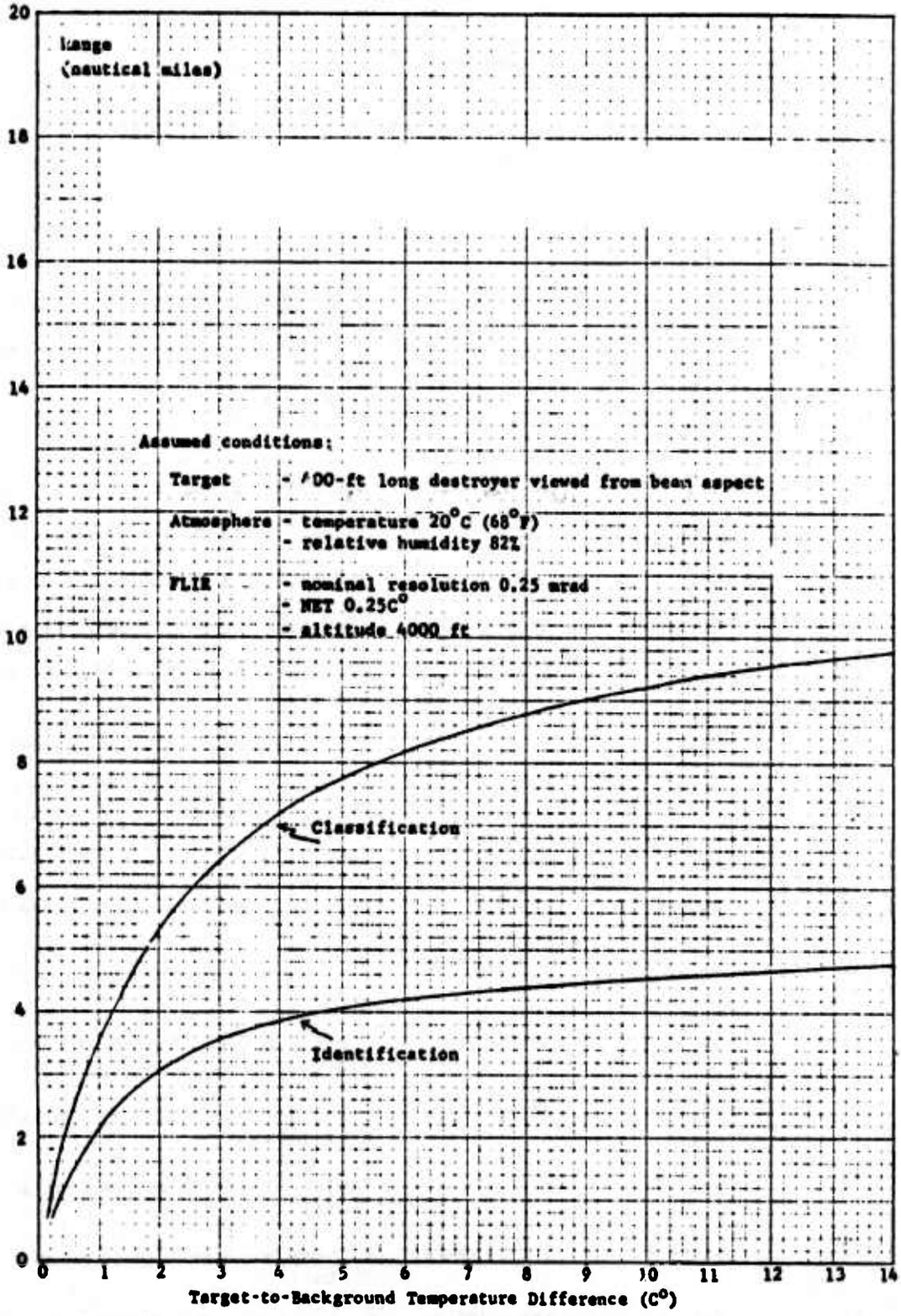

Fig. 22 — Target classification and identification ranges as a function of target-to-background temperature difference

Table I
Site Locations and Descriptions

SITE NO.	LATITUDE	LONGITUDE	SITE DESCRIPTION
1	56 N-Coast	151-157 W	Kodiak, Alaska (NE Pacific Ocean)
2	45-47 N	53-56 W	Argentia, Newfoundland (Atlantic Ocean SE of Newfoundland)
3	42 N-Coast	66 W-Coast	Boston, Mass. (Atlantic Ocean E of central Mass.)
4	39.7 N	129.4 E	Wonsan, North Korea (Sea of Japan)
5	38-40 N	72 W-Coast	Atlantic City, N.J. (Atlantic Ocean E of S N.J., Del. and N Md.)
6	36-38 N	Coast-126 W	San Francisco, Calif. (Pacific Ocean S and W of central Calif.)
7	37.9 N	25.1 E	South Aegean Sea (E of Athens, Greece)
8	36.0 N	3.4 W	Malaga, Spain (W end of Mediterranean)
9	36.0 N	133.2 E	Matsue, Japan (S end of Sea of Japan)
10	32.2 N	33.3 E	Port Said, Egypt (SE Mediterranean)
11	27.2 N	50.2 E	NW Persian Gulf (between Saudi Arabia and Iran)
12	25.0 N	57.8 E	N Gulf of Oman (between Iran and Oman)
13	23-25 N	79-83 W	Key West, Fla. (Gulf of Mexico & Atlantic Ocean between Florida & Cuba)
14	29.9 N	67.8 E	Karachi, Pakistan (N Arabian Sea)
15	20.4 N	158.3 W	Hawaiian Leeward (Pacific Ocean S of Oahu)
16	18-20 N	74-76 W	Guantanamo, Cuba (Caribbean S of E Cuba)
17	17-22 N	110 E-Coast	S China Sea Area VII (E of North Vietnam)
18	17.9 N	85.2 E	Vishakhapatnam, India (Bay of Bengal E of S India)
19	14.2 N	73.0 E	Panjim, Goa (Arabian Sea W of S India)
20	11-14 N	111 E-Coast	S China Sea Area I (E of South Vietnam)
21	7-11 N	102 & 103 E-Coast	S. China Sea Area VI (Gulf of Siam adjoining Malaysia)

MAY

PERIOD: (PRIMARY) 1951-1968
(OVER-ALL) 1864-1968

AREA 004 BOSTON
42N-COAST 66W-COAST

TABLE 13

PERCENT FREQUENCY OF RELATIVE HUMIDITY BY TEMP

TEMP F	0-29	30-39	40-49	50-59	60-69	70-79	80-89	90-100	TOTAL OBS	PCT FREQ
85/89	.0	.0	.1	.0	.0	.0	.0	.0	1	.1
80/84	.0	.0	.1	.1	.0	.0	.0	.0	2	.1
75/79	.0	.0	.1	.0	.0	.0	.0	.0	1	.1
70/74	.1	.1	.0	.0	.1	.0	.0	.0	3	.2
65/69	.1	.1	.1	.3	.2	.2	.0	.0	17	1.0
60/64	.0	.0	.2	.3	.5	.4	.3	.1	32	1.8
55/59	.0	.0	.2	.4	1.0	1.7	1.6	1.6	112	6.5
50/54	.0	.0	.1	.3	1.2	3.3	7.0	7.1	330	19.0
45/49	.1	.1	.2	.5	1.6	5.6	13.7	16.0	656	37.8
40/44	.0	.2	.1	.1	1.6	4.1	10.3	13.4	517	29.8
35/39	.0	.0	.0	.1	.1	.2	.9	2.3	63	3.6
30/34	.0	.0	.0	.1	.0	.0	.0	.0	1	.1
TOTAL	5	8	18	38	105	272	585	704	1735	100.0
PCT	.3	.5	1.0	2.2	6.1	15.7	33.7	40.6		

TABLE 14

PERCENT FREQUENCY OF WIND DIRECTION BY TEMP

N	NE	E	SE	S	SW	W	NW	VAR	CALM
.0	.0	.0	.0	.0	.0	.0	.1	.0	.0
.1	.0	.0	.0	.1	.0	.0	.0	.0	.0
.0	.0	.0	.0	.1	.0	.0	.0	.0	.0
.0	.0	.0	.0	.1	.0	.1	.1	.0	.0
.0	.0	.0	.1	.2	.3	.2	.2	.0	.0
.1	.1	.2	.1	.7	.3	.2	.1	.0	.0
.4	.4	.7	.5	2.2	1.0	.6	.5	.0	.1
1.1	1.9	1.4	1.8	4.3	3.8	2.9	.9	.0	.9
1.8	2.9	3.3	3.8	7.7	8.1	5.8	3.1	.1	1.2
2.7	2.1	2.4	3.1	4.5	5.7	4.6	3.7	.0	1.2
.4	.3	.5	.3	.7	.3	.7	.4	.0	.0
.0	.0	.0	.0	.0	.0	.0	.1	.0	.0
114	133	146	167	356	340	260	158	1	60
6.6	7.7	8.4	9.6	20.5	19.6	15.0	9.1	.1	3.5

TABLE 15

MEANS, EXTREMES AND PERCENTILES OF TEMP (DEG F) BY HOUR

HOUR (GMT)	MAX	99%	95%	50%	5%	1%	MIN	MEAN	TOTAL OBS
00&03	76	61	55	46	39	36	33	46.5	605
06&09	64	57	54	46	39	38	36	46.5	497
12&15	79	63	58	47	40	37	34	46.2	771
18&21	85	70	62	48	40	38	34	49.5	804
TOT	85	66	57	45	38	36	33	47.3	2677

TABLE 16

PERCENT FREQUENCY OF RELATIVE HUMIDITY BY HOUR

HOUR (GMT)	0-29	30-59	60-69	70-79	80-89	90-100	MEAN	TOTAL OBS
00&03	.0	.2	1.2	3.0	8.8	9.8	87	401
06&09	.1	.2	.6	2.5	5.7	9.3	88	320
12&15	.0	.9	1.4	4.1	9.4	11.8	86	480
18&21	.2	2.5	2.8	6.1	9.9	9.5	81	540
TOT	5	64	105	274	589	704	85	1741

Fig. 23 — Representative page of data for Boston, Massachusetts, in May reproduced from Naval Weather Service Command summary of synoptic meteorological observations

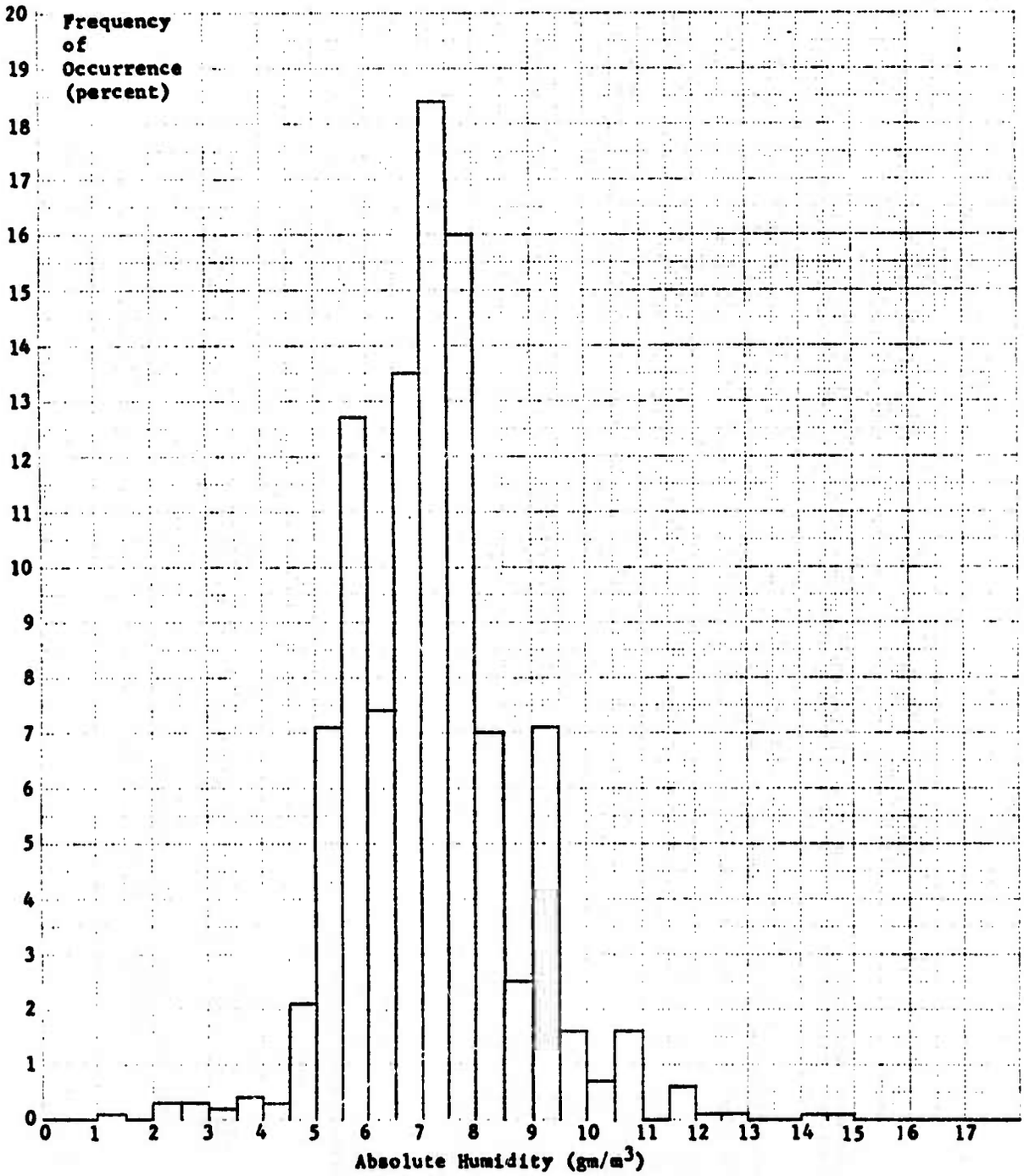

Fig. 24 — Percent frequency of occurrence of given values of absolute humidity for Boston in May

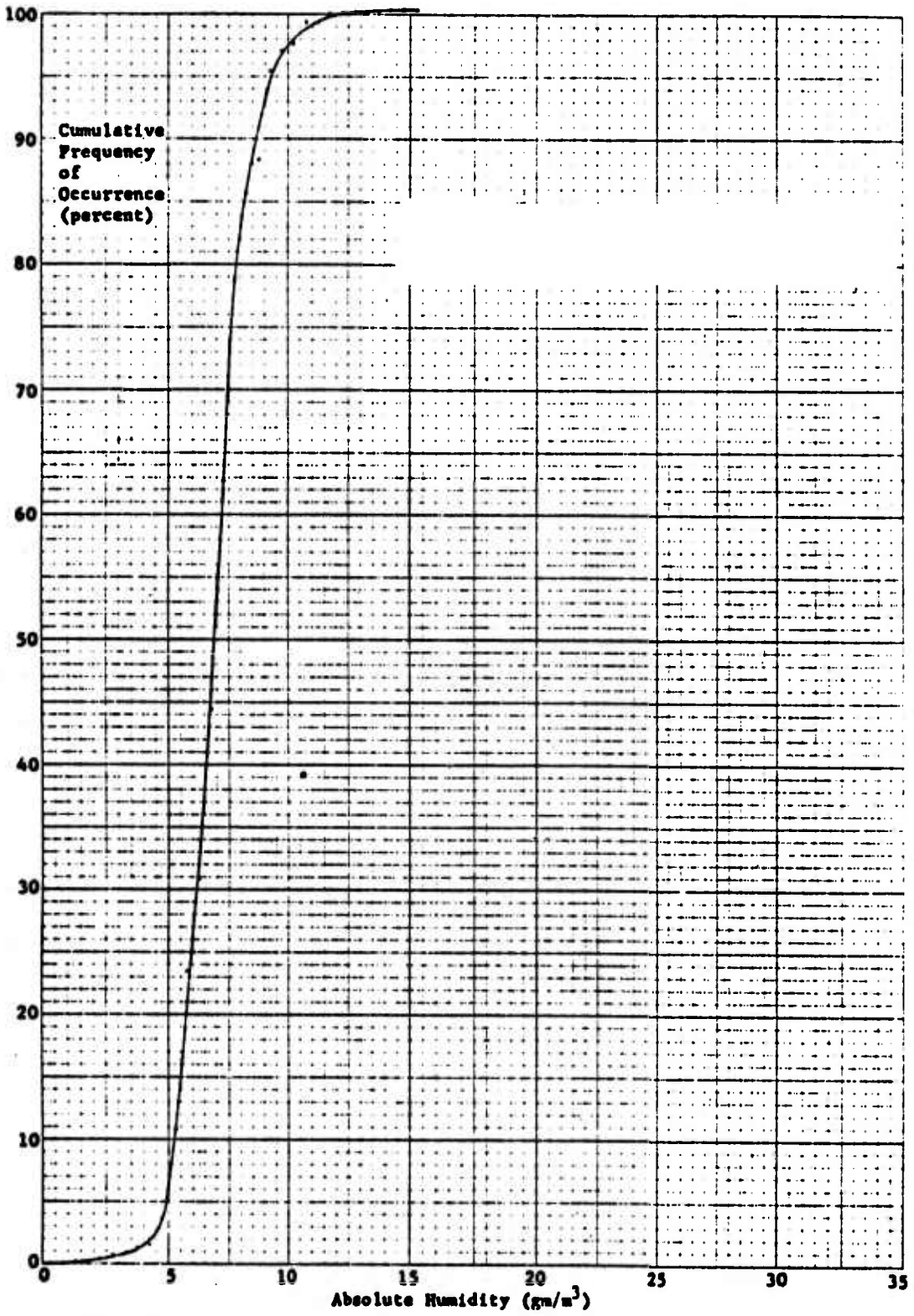

Fig. 25 — Cumulative frequency of occurrence of given concentrations of atmospheric water vapor for Boston in May

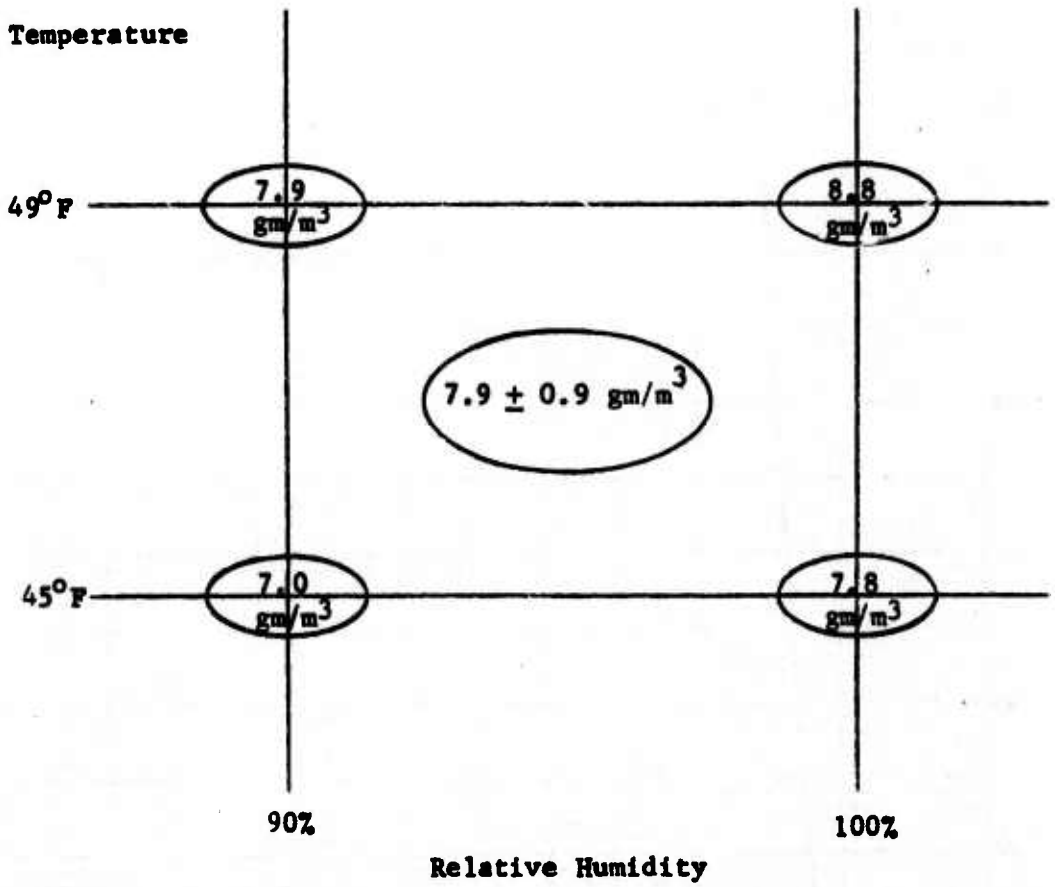

Fig. 26 — Values of absolute humidity corresponding to each of the four "corners" of a representative relative humidity — temperature interval

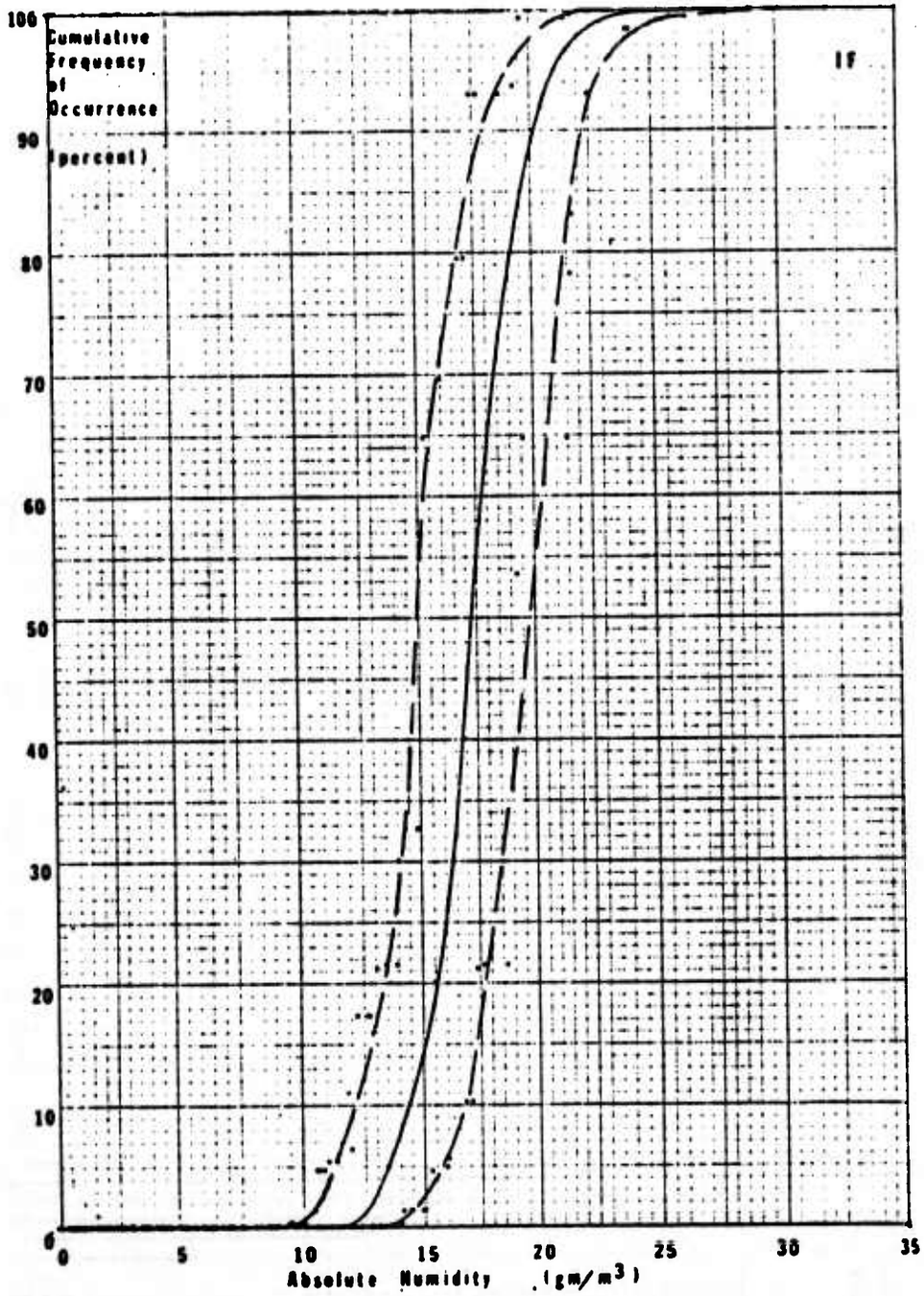

Fig. 27 — Cumulative frequency of occurrence of given concentrations of atmospheric water vapor for "Port Said" in June

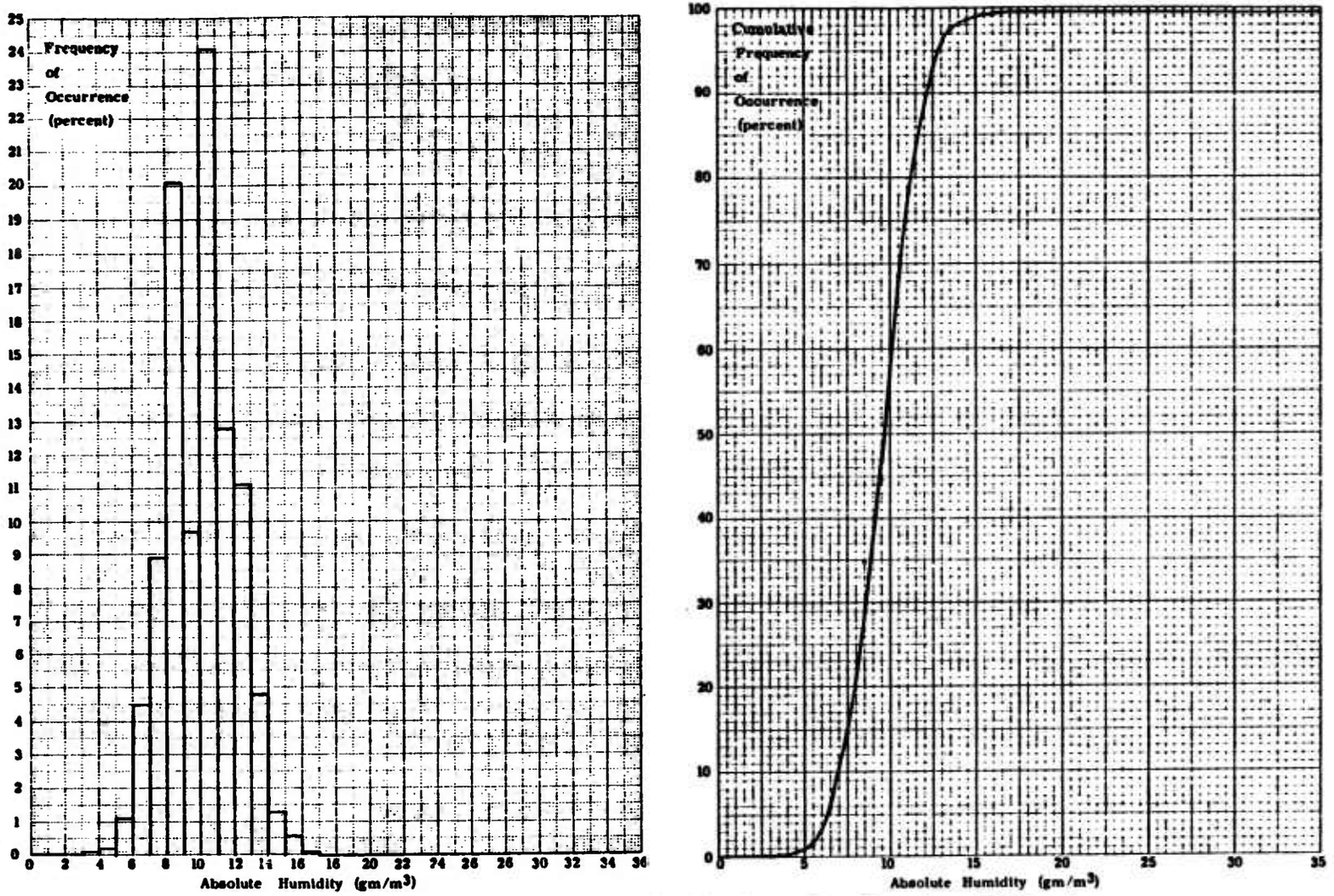

Fig. 28 — Annual absolute humidity distribution — San Francisco, California

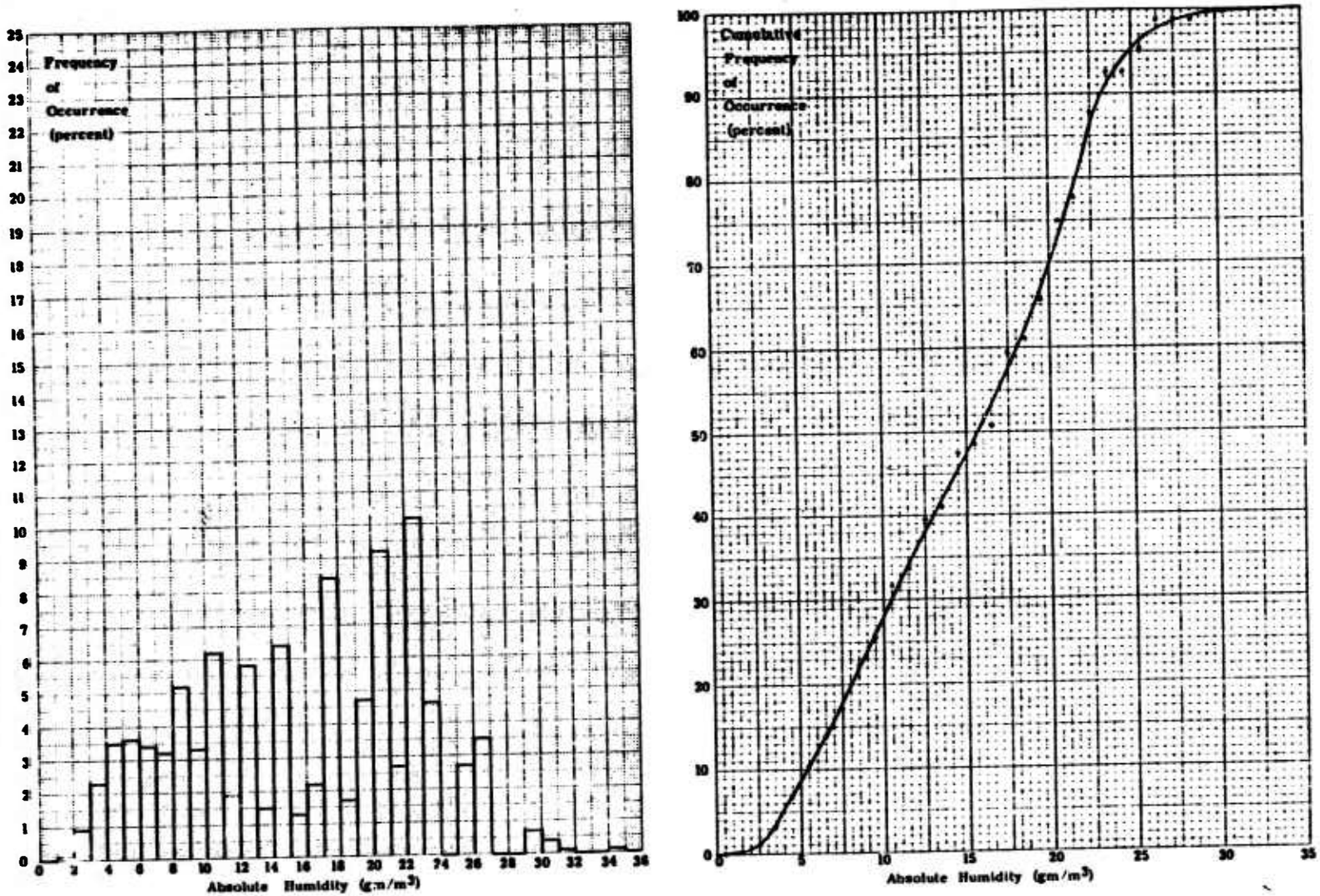

Fig. 29 — Annual absolute humidity distribution — composite of 21 sites

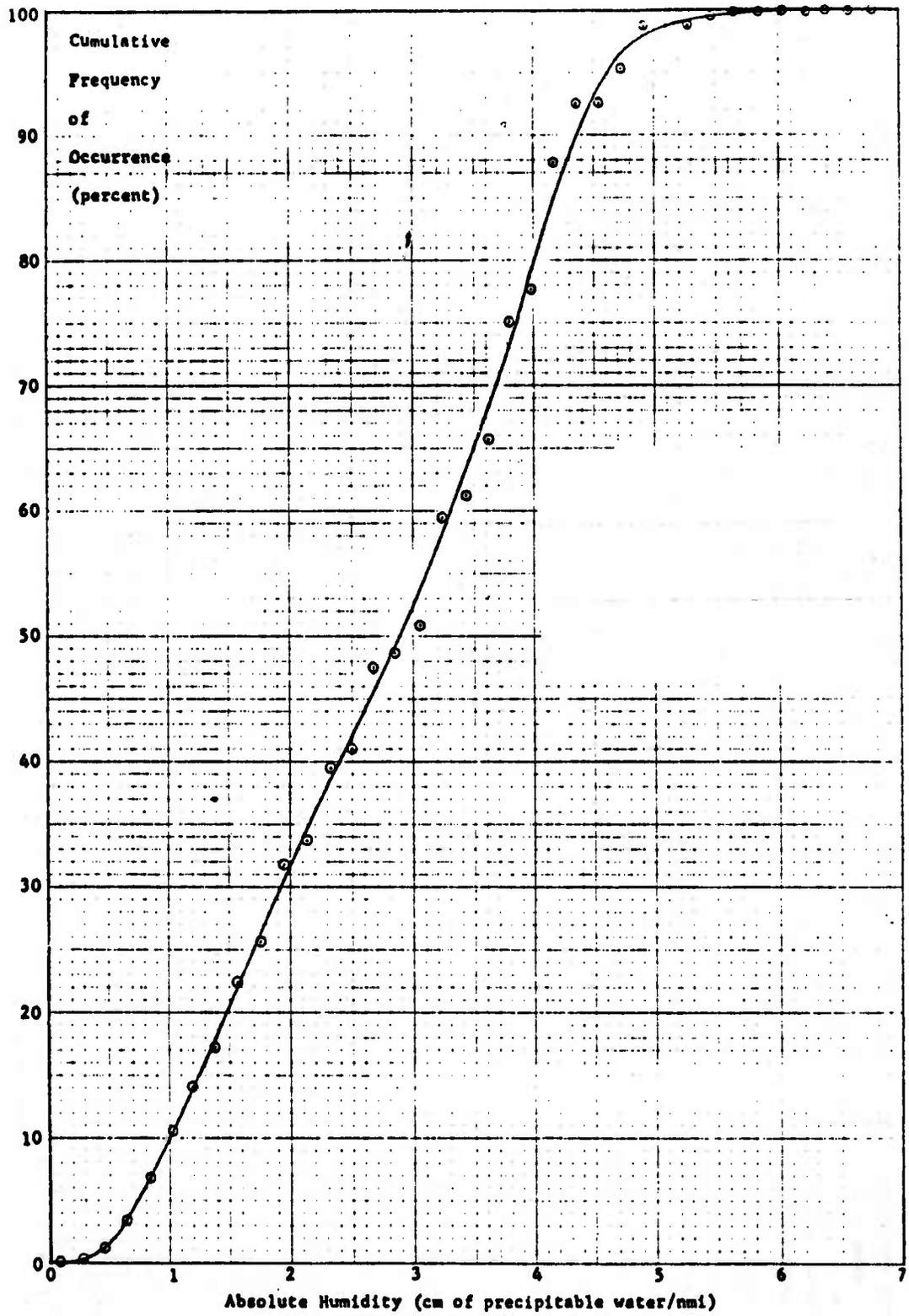

Fig. 30 — Composite annual cumulative frequency of occurrence of given concentrations of atmospheric water vapor for 21 selected marine locations

22 Feb 2017

MEMORANDUM FOR THE RECORD

FROM: Division Director EO & Special Mission Sensors, Avionics, Sensors and E* Warfare Dept (AIR 4.5.6)

TO: Office of Counsel, Naval Air Warfare Center, Aircraft Division (NAWCAD)

Subj: SECURITY RECOMMENDAION FOR FOIA REQUEST, DON FOIA CASE FILE NUMBER 2015-008952

Ref: (a) SECNAVINST 5720.42F, DON FOIA Program, 06 Jan 99

(b) Executive Order 13526

1. Releasable Recommendations. The following documents were reviewed by AIR 4.5.6. Each of the following documents were found to be releasable in their entirety:

    a. Document (1) of Subj. NAVAIRDEVCEN Report No. NADC-AW-L5902, 24 Mar 1959, "Investigation of a Towed-capsule Installation of the AN/ASH-2 Condensation Nuclei Detector" (ADB966296)
    b. Document (10) of Subj. NAVAIRDEVCEN Report No. NADC-AW-N6302, 4 Apr 1963, "Maritime Applications of Infrared Mapping Systems" (AD-359080L)
    c. Document (16) of Subj. NAVAIRDEVCEN Report No. NADC-AE-6759, 16 Jan 1968, "Modified Reconofax VI Infrared Mapping Set with Real Time Inflight Display" (AD-387513)
    d. Document (17) of Subj. NAVAIRDEVCEN Report No. NADC-AE-6828, 12 Nov 1968, "Modified AN/AAD-2(XE-2) Infrared Detecting Set with Real-Time Inflight Display (AD-500493)
    e. Document (18) of Subj. NAVAIRDEVCEN Report No. NADC-72167-AE, 10 Apr 1973, "Index of Performance for FLIR (Forward Looking Infrared) Imaging Devices" (AD-525116)

2. Partially Releasable Recommendations. AIR 4.5.6 recommends pages 27 through 68 are releasable the following report: Document (20) of Subj. Naval Research Laboratory Memorandum Report 3240, Proceedings of the Electro-Optics/Meteorology Meeting on 7 Aug 1975, Mar 1976 "FLIR Performance Modelling and its Dependence upon Climatology and Meteorology "(AD-D516929L). All other data in this report is not under the technical authority of AIR 4.5.6.

3. [redacted]

4. Basis of Recommendation. All information was reviewed with current class guides and what is considered open source information. Appropriate recommendations made above with respect to findings. Documents found with portions releasable were sanitized based on class guides and reference (b). Such disclosure of Department of the Navy classified information would give potential adversaries insight that would present a significant threat to national security.

5. Exemptions Utilized. Two separate exemptions were utilized in the determination of what information should be sanitized or exempted from release via Freedom of Information Act (FOIA) request process. All current Classified Military Information (CMI) has been sanitized out of the document under FOIA Exemption 1, Executive Order 13526 Section 3.3(4). This Executive Order Section covers CMI that was originally classified over 25 years ago from date of this memorandum. Subject matter experts within AIR 4.5.6 were utilized in making the exemption determinations.

6. Point of Contact. The point of contact for this security review and recommendation is Mr. Paul W. Reimel, AIR 4.5.6 Division Director, paul.reimel@navy.mil, 301-342-0100.

2/28/2017

X Paul W. Reimel

Paul W. Reimel

Signed by: REIMEL.PAUL.W.1229241016

Distribution:

NAWCAD 7.4

NAWCAD 4.5.6